UNIVERSITY of CALIFORNIA
Santa Barbara

Dynamics of Immune System Vulnerabilities

A dissertation submitted in partial satisfaction of the
requirements for the degree of

Doctor of Philosophy

in

Physics

by

Sean P. Stromberg

Committee in charge:

Professor Jean M. Carlson, Chair
Professor Everett A. Lipman
Professor Boris I. Shraiman

December 2009

The dissertation of Sean P. Stromberg is approved:

Professor Everett A. Lipman

Professor Boris I. Shraiman

Professor Jean M. Carlson, Chair

September 2009

Dynamics of Immune System Vulnerabilities

by

Sean P. Stromberg

To my mother who should have lived to see this, my wife who got me through it, and the child we are expecting who I hope to share it with.

Acknowledgements

Thanks to so many people. First and foremost, Jean Carlson the most supportive, nurturing and exciting professor I could have hoped for. She looks for creative independent students interested in important problems and gives them the support they need, not just financial and academic support, but personal support as well. I believe she makes the success of her students her top priority.

The research in Jean's group is diverse, creative and exciting, and working in that environment helped develop the ideas in this dissertation. Ted Brookings who studied networks, scaling and neuroscience in the group, is an oracle of knowledge and helped me solve many computational problems[1]. Morgan Page worked on inversion problems in earthquakes, had a gift for outreach and explaining complicated things simply, and in an exciting manner always took time for a break and a game or two of pente when I needed it[2]. Lisa Manning, whose work on amorphous glassy materials should prove transformative, is as gifted a chef as she is a scientist. Eric Daub has applied methods from amorphous materials to the study of earthquakes[3]. Kevin Brown, a post-doc working on neuroscience in the group, has provided great friendship, academic career advice and scientific knowledge[4]. Ann Hermundstad, who is working on neuroscience, gets the prizes

[1] with a cold and dry sense of humor and a bow made of office supplies
[2] I think she solved connect four
[3] and makes the greatest beer any of us have ever tried
[4] and tips on what music I should be listening to

for office-mate awesomeness and good music sharing. And Nada Petrovic who is nobly working on models of optimal policy in disaster response has also added to the friendly and exciting atmosphere.

The research groups of Rustom Antia at Emory University and Alan Perelson at Los Alamos National Lab, both in theoretical immunology, have hosted me for short periods. This has been very helpful in improving my understanding of how the immune system works, yielding new ideas for research projects, and helping me to gauge the importance of this work. Andy Yates now at Albert Einstein has been very supportive, often helping me with problems remotely. John Doyle at Caltech and Frank Doyle[5] at UCSB also provided ample help, advice and enthusiastic support in helping me find a postdoctorial research position.

I could not have gotten here or completed this without the help of my family. My mother always wanted me to express my creative side and I hope this work would have pleased her in that respect. My wife has been supportive from start to end and has made many sacrifices. She also happens to be the life sciences librarian at UCSB[6] and she deserves to be recognized for all the help she has given me in finding the information I need on different topics in immunology, and often brings to my attention new books on the subject I would not have otherwise known about. My belief that you don't need a membership card or

[5]no relation

[6]the list of immunology texts has probably doubled in the last year

formal training in something to jump right in and start working on it comes from my father, and I never would have worked on immunology without that. He has always loved science and I know this makes him proud[7]. My mother-in-law Carolyn sends me cookies routinely and I'm sure she can't wait to see this cookie-fueled manuscript. And my aunt Cheri always told her daughters she wanted a doctor in the family... I consider that support. Gramps, don't worry about the chapter on immunosenescence; this only happens to people who age.

Jack, Jim, Chris, Hadrian, Felix, Tikhon, Feraz, Chizu, Melanie and Jean-Luc provided friendship and hilarious and thoughtful conversation at UCSB. Shammi, Jen, Mike, Woody, Sonya, Tobi, Tim, Greta, Kevin and Sam provided the same in places other than UCSB. Several children and adolescents with an interest in science have inspired me to set a good example as a scientist. They are Devlin Ott, Damian Herlevic, Evan Penner and Carolyn Mathieu.

I am also indebted the other members of my thesis committee: Boris Shraiman, and Everett Lipman, for considering my work. Boris and Frank Doyle also designed three courses at UCSB on theoretical biology that I had the pleasure of taking[8]. Don Marolf worked hard to improve the grad-student experience.

This work was supported by the David and Lucile Packard Foundation and the Institute for Collaborative Biotechnologies through the United States Army.

[7] Dad, if you ever read this let me know and I'll buy you dinner...

[8] these were the best classes I took at UCSB

Curriculum Vitæ

Sean P. Stromberg

Education

2009	PhD in Physics, University of California, Santa Barbara
2006	MA in Physics, University of California, Santa Barbara
2000	BS in Physics, University of California, Santa Cruz

Research and Industrial Experience

2004-Present	Graduate Student Researcher, UCSB Complex Systems and Institute for Collaborative Biotechnologies
2003-2004	Graduate Student Researcher, UCSB High-Energy Experiment
2001-2002	Materials Scientist/Engineer, Lawrence Berkeley National Laboratory
2000-2001	Quality Assurance/Service Engineer, Xenogen Corp.

Teaching

2008-2009	Science Fair Mentor, Carolyn Mathieu
2002-2004	Teaching Assistant, UCSB
2000	Math and Science Tutor, Palomar College, San Marcos, CA

Organizational

2007-Present	UCSB Physics Gradlife Committee Co-Chair
2007-2008	Gradloquium Founder and Coordinator, UCSB
2005	Organizer for Union of Concerned Scientists Panel on Scientific Integrity

Publications

"The Suppression of Immune System Disorders by Passive Attrition" S. P. Stromberg and J. M. Carlson, *PLoS One*, Submitted

"Pathogen Induced Tolerance," S. P. Stromberg and J. M. Carlson, *PLoS One*, In Revision

"Robustness and Fragility in Immunosenescence," S. P. Stromberg and J. M. Carlson, *PLoS Computational Biology*, 2006

"The assembly of the silicon tracker for the GLAST beamtest engineering model," Allport P, Atwood E, Atwood W, et al., *Nucl. instrum. methods phys. res. sect. A*,: 466(2), p376-382 (2001).

"The silicon tracker of the beam test engineering model of the GLAST large-area telescope,", Atwood E, Atwood W, Bhatnager B, et al., *Nucl. instrum. methods phys. res. sect. A*,: 457(1-2), p126-136 (2001).

"Measurement of dose rate dependance of radiation induced damage to the current gain in bipolar transistors," Dorfan D, Dubbs T, Grillo AA, et al., *IEEE Trans. Nucl. Sci.*, 46(6), p1884-1890 (1999).

Honors and Awards

2007	UCSB Physics Department Recognition of Gradlife Service
2007	Boulder School for Condensed Matter Physics, Scholarship
2006	Time Magazine Person of the Year
1998-1999	University of California Regents Scholarship

Abstract

Dynamics of Immune System Vulnerabilities

by

Sean P. Stromberg

The adaptive immune system can be viewed as a complex system, which adapts, over time, to reflect the history of infections experienced by the organism. Understanding its operation requires viewing it in terms of tradeoffs under constraints and evolutionary history. It typically displays "robust, yet fragile" behavior, meaning common tasks are robust to small changes but novel threats or changes in environment can have dire consequences.

In this dissertation we use mechanistic models to study several biological processes: the immune response, the homeostasis of cells in the lymphatic system, and the process that normally prevents autoreactive cells from entering the lymphatic system. Using these models we then study the effects of these processes interacting.

We show that the mechanisms that regulate the numbers of cells in the immune system, in conjunction with the immune response, can act to suppress au-

toreactive cells from proliferating, thus showing quantitatively how pathogenic infections can suppress autoimmune disease. We also show that over long periods of time this same effect can thin the repertoire of cells that defend against novel threats, leading to an age correlated vulnerability. This vulnerability is shown to be a consequence of system dynamics, not due to degradation of immune system components with age.

Finally, modeling a specific tolerance mechanism that normally prevents autoimmune disease, in conjunction with models of the immune response and homeostasis we look at the consequences of the immune system mistakenly incorporating pathogenic molecules into its tolerizing mechanisms. The signature of this dynamic matches closely that of the dengue virus system.

Contents

List of Figures

List of Tables

Chapter 1

Introduction

Observations of the adaptive immune system trace back to the Peloponnesian war in the fifth century BCE. In his *History of the Peloponnesian War* Thucydides describes in epic and gory detail, a plague that consumed nearly a third of the population of Athens. In this plague the doctors were the first to die as they were exposed to the disease most often. This left the population with the choice of abandoning their sick loved ones, leaving them to face death on their own, or bring them comfort and risk death themselves. At this time immunity was discovered and so was the specificity of the protection it conferred (from the translation by Richard Crawley):

> "Yet it was with those who had recovered from the disease that the sick and the dying found most compassion. These knew what it was from experience, and had now no fear for themselves; for the same

> man was never attacked twice- never at least fatally. And such persons not only received the congratulations of others, but themselves also, in the elation of the moment, half entertained the vain hope that they were for the future safe from any disease whatsoever."

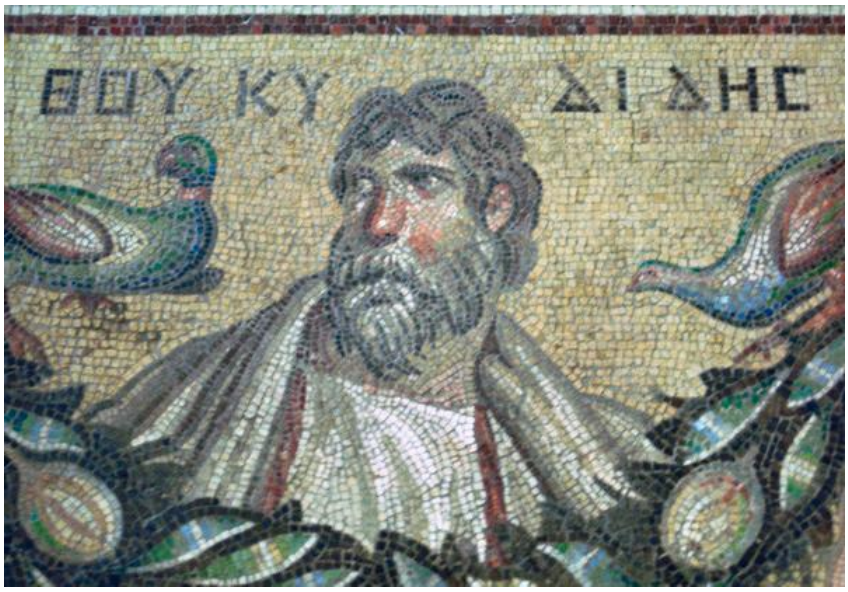

Figure 1.1: Tile Mosaic of Thucydides from the Altes Museum, Berlin

After the discovery of immunity in 430 BCE it took until the fifteenth century before the first recorded attempts to exploit this dynamic with what we now call vaccination. These vaccinations involved inhaling, or the rubbing into small cuts in the skin, the dried crusts from pustules caused by smallpox infection. The virus contained in the dried pustules was normally in an attenuated form yielding less severe disease, an immune response, and immunity to future exposures of the

disease... but not always. Frequently this type of vaccination would result in full blown smallpox infection and death.

In 1798 Edward Jenner, having noticed that milk maids rarely contracted small pox made the connection that their frequent exposure to cow pox provided them with immunity to smallpox. He then inoculated an eight year old child with the crust from a pustule of cow pox infection, and later intentionally infected him with smallpox to prove the vaccine provided immunity. This is the origin of the term vaccine coming from the latin word for cow, *vacca*. In the time since the smallpox vaccine was developed there have been vaccines developed for 28 other diseases[1], the most recent being the human papilloma virus.

While this original technique of using attenuated or biologically inactivated virus to stimulate a small immune response has proved an extremely useful technique, the development process has conceptually changed very little from Jenner's time. The method of guess and check for vaccine development is still the heart of this science. With the addition of orphans', prisoners', and poor peoples' rights since Jenner's time, this has made vaccine development a very slow and cautious practice. While this procedure is fine for developing vaccines for many infectious diseases, for critical disease epidemics such as swine flu, vaccine design would be aided by theoretical methods.

[1]There are additional vaccines for subspecies of these viruses such as different strains of influenza

Figure 1.2: Edward Jenner administering first smallpox vaccine to James Phipps. James' father standing to his left was a servant of Jenner's. Painting by Gaston Melingue.

Electronics development provides an analogy showing the utility of mechanistic theoretical models. In this field there is little guess work, and what guess work there is, normally is performed with computer simulations aided by mathematical models. Once a design satisfies necessary parameters a prototype is developed and checked against the theory. Having theoretical models also aids in diagnosing problems not realized until prototype construction.

Initially the mathematical models used in the design of electronics with transistors were based on very complex empirical models. Simulations using these

models were slow and the models could not be extended beyond the limits of the experiments used to fit the empirical curves. Device physicists then began constructing mechanistic models based on the underlying physics of the transistor. This solved both the problem of limits of experimental observation with empirical models, as mechanistic models can be extended beyond data, but also the problem of slow simulations due to mechanistic models yielding approximations and describing the limits of where these approximations are valid. The work of this dissertation is an effort to increase the theoretical and mechanistic understanding of how the immune system works.

Much of the mathematical modeling consists of systems of differential equations. The differential equation lets us describe how a physical system changes in time. Formulating the dynamics of a system in terms of rules for how they change rather than their specific behavior allows a single equation to describe many different types of phenomena. The differences between these phenomena arise from varying initial conditions. Newton's single differential equation for projectile motion describes both how an object falls to the ground and the orbital motion of satellites, the difference in behaviors coming from the initial positions and momenta of these objects. Likewise, the models of this dissertation show illness and immune response, immunity, hemorrhagic fevers, and immunosenescence coming from the same system with different starting conditions at the time of infection.

We also make use of some stochastic simulation techniques. Stochastic simulation techniques are used in systems where large variability from system to system even with identical starting conditions. In contrast to differential equations which give a deterministic output, stochastic equations give a probabilistic one. Stochastic simulations make use of pseudo-random number generators on computers. When the reactions of a system are characterized by statistical distributions, or statistical properties like mean and variance, these simulation techniques extrapolate from the individual reactions to variability of the system as a whole.

Developing theoretical models in this manner, either deterministic or otherwise, for immune system behavior gives the ability to quantitatively calculate dynamics that can not be easily observed. It generates ideas for new experiments to help resolve ambiguity in the underlying mechanics. It makes explicit the reactions that are taken into account allowing us to resolve the quantitative importance of different mechanisms in system behavior. The development of theoretical models of immune system dynamics has also been used to generate optimal treatment strategies for different diseases.

The immune system is an ideal example for the study of complex systems. It offers adaptation and evolution on observable time scales and offers testable hypotheses. In response to diseases the immune system is adapting to its environment. Molecular evolution of antibody molecules is approximately one-thousand

times faster than other genes in the body and can be observed during an immune response.

Chapter 2 of this dissertation shows that responses to infectious diseases affect immune system disorders such as allergies and autoimmune disease. It shows that the mechanisms which prevent immune system cancers, when taken in conjunction with pathogen exposure, also provide a mechanism to suppress autoimmune disease. This provides quantitative answers to common concerns regarding hygiene in the home, and an explanation for the prevalence of autoimmune and allergic disorders in developed nations that doesn't exist in developing nations.

Chapter 3 looks at the same mechanisms from Chapter 2 and extrapolates over very long times. This looks at the suppressive effect from Chapter 2 applied to the small populations of cells that are needed to fight infectious diseases that the system has never seen before. This shows a small number of cells left in old age to fight new diseases but many memory cells left for fighting recurrences of common diseases. This is an example of "Highly Optimized Tolerance" (HOT), and the system is observed to over adapt with age to fighting common diseases leaving an aged immune system vulnerable to rare and never before observed diseases. This provides some explanation as to why the elderly can suffer symptoms like encephalitis when exposed to west nile virus while others have asymptomatic infections.

Chapter 4 also looks at the suppressive mechanisms from Chapter 2 and combines them with another mechanism that eliminates autoimmune disease called negative selection. Negative selection provides tolerance to the bodies own chemicals by eliminating lymphocytes (the cells of the immune system) that would respond to these chemicals. We then look at what happens when the chemicals from pathogen take place in the negative selection reaction thus tolerizing parts of the immune system to future pathogenic infections. The signatures of this mechanism are shown to be in close agreement with those of the dengue virus system.

It is expected that this work and the work built on it will help fight pathogenic diseases and aid in the prevention of the diseases the immune system itself causes. These techniques provide a complimentary approach to classical immunology.

Chapter 2

The Suppression of Immune System Disorders by Passive Attrition

2.1 The Hygiene Hypothesis

The immune system provides protection from diseases ranging from intestinal parasites to viruses and even cancers. The immune system is also the cause of many other types of disease, like autoimmune diseases and allergies. There is a large body of evidence, ranging from epidemiological to animal model experiments, showing that exposure to the diseases that the immune system fights

provides protection from the diseases that the immune system causes. The paradoxical protection conferred by pathogenic infections against immune system disorders is often referred to as the "Hygiene Hypothesis" [1, 2]. Understanding the mechanisms of this protection has important clinical consequences.

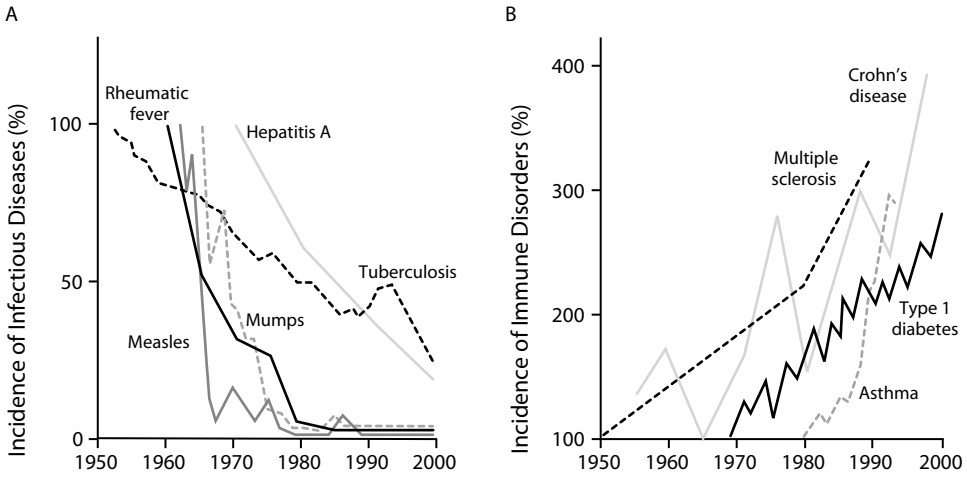

Figure 2.1: Panel A shows data on infectious diseases. Panel B shows data on immune disorders. The anti-correlation is shown to be causal. This figure was reproduced with permission from Bach, J.F. *The Effect of Infections on Susceptibility to Autoimmune and Allergic Diseases*(2002), N Engl J Med Vol. 347, No. 12 Copyright ©*2002 Massachusetts Medical Society. All rights reserved.*

Though some infectious diseases have been shown to cause autoimmune disease, this is not a general feature of infectious disease. The large body of evidence showing the suppression of autoimmune and allergic disease by infection, is reviewed in Bach (2002) [2]. The evidence of this effect is seen in three major categories:

- The dramatic increase in incidence of autoimmune diseases over the last 50 years coinciding with a decrease in many infectious diseases. This is shown in Figure 2.1 copied from Bach (2002)[2].

- A trend of higher incidence of autoimmune and allergy with higher incomes and lower temperatures,[1]

- An anti-correlation between infection history and autoimmune incidence.

2.1.1 Alternate Hypotheses

One might consider hypotheses other than suppression by infections to explain observed regional trends in immune system disorders. These might include regional differences in diagnostic capabilities, genetics, and other environmental factors besides pathogen frequency.

While diagnostic capabilities can vary from region to region, two of the most studied autoimmune diseases in this field are multiple sclerosis and type 1 diabetes mellitus. These diseases are not often misdiagnosed. Additionally it has been observed that asthma and type 1 diabetes are more prevalent in first born children unless the children attended daycare[3, 4]. There should be no diagnostic

[1]Bacterial proliferation is inhibited by lower ambient temperature decreasing the likelihood of infection. Lower temperatures also prevent transmission of some tropical viruses, as the mosquitos needed for transmission can not survive the cold climate. Increased income yields stricter control of microbes in food and water and provides better housing conditions.

difference in these groups, only a difference in exposure rates from other children.

It is possible that genetic factors may give some differences in incidence of immune disorders, but these factors are unable to explain the rapid increase in autoimmune diseases over the last 50 years. The increase is 3-4 fold over the last 50 years for type 1 diabetes, asthma, multiple sclerosis, and Crohn's disease. A more direct study of genetic factors looked at children of recent immigrants from Pakistan to the United Kingdom. The study showed that the children of recent immigrants have the same incidence of type 1 diabetes as non-immigrants, ten times the incidence in Pakistan[5, 6].

Environmental factors other than infectious diseases are controlled for in the study of first born children mentioned above. This assumes that the only environmental difference is exposure to infection by older siblings. Another study that controls for some regional environmental factors is a study of children in areas where farmers and non-farmers both live. Here it was seen that children growing up on farms are less likely to suffer from allergies than their non-farming neighbors are[7].

Animal experiments directly control for these factors and show that exposure to foreign antigen suppresses autoimmune disease. Non-obese diabetic (NOD) mice are observed to be twice as likely to develop diabetes in isolated sterile conditions than are genetically identical mice in a conventional environment[8]. A

similar result was obtained from studies of induction of experimental autoimmune encephalomyelitis (EAE) in Lewis rats. The rats raised in a conventional environment typically showed no response to the EAE priming agent[9]. The direct effects of foreign antigen are also studied in animal models. Exposure of lupus prone mice to either lactate dehydrogenase-elevating virus or malaria prevents lupus, and treatment with killed bacteria offers protection from diabetes in NOD mice.

2.1.2 Proposed Mechanisms

There are many proposed mechanisms by which infections might suppress autoimmune disease. The hypotheses receiving the most attention are: Th1/Th2 balance, generation or activation of Regulatory T cells, and competition between cells for homeostatic survival factors (the major study of this chapter).

It had been suggested that as Th1 cells and Th2 cells each have a suppressive effect on each other, a system out of balance might result in one cell type being unregulated by the other. Th1 cells are implicated in autoimmune diseases while Th2 cells are a component of allergic disease. If Th1/Th2 balance is the mechanism generating a suppression of immune system disorders, we expect allergy and autoimmune incidence to be inversely correlated. This is not the case however. Individuals with diabetes or rheumatoid arthritis have been observed to have a

higher incidence of atopic disease[10, 11].

Bystander suppression by regulatory T cells in response to infections is a compelling hypothesis. These cells have many possible mechanisms of suppression and characterization of these cell types is still in its infancy. It has been shown that the suppressive effects conferred by killed bacteria persist in IL-10 and IL-4 knockout NOD mice[12]. These suppressive cytokines are only two of the several possible mechanisms that regulatory T cells may be using to suppress immune system disorders.

In this paper we study the competition between cells for homeostatic survival factors. Competition for survival factors has been previously studied in the context of new memory cells being added to the memory population after infection. This raises the total number of memory cells beyond what the niche can support. With no cell having a competitive advantage with regard to homeostasis, all subpopulations will decrease in number at the same rate until the system returns to homeostasis. This is the mechanism for passive attrition of a clone of specific memory cells to a non cross-reactive heterologous infection.

Infectious diseases have also been shown to directly trigger certain autoimmune diseases [13]. This however is not a general feature of infectious diseases and we do not consider this effect here. If this were a common feature the normal infection rate of people getting sick once or twice a year would result in autoimmune disease

being the norm and not the exception. It would also be in strong contradiction to the observations of Fig. 2.1.

2.2 General Homeostatic Regulation

Homeostatic regulation in the immune system refers to the mechanisms that control the number of cells in the system. Without homeostatic regulation cells would either experience unconstrained growth (cancer), or decay to extinction.

We first present a general model of homeostasis without explicit definition of the regulatory mechanisms. This technique was previously used by Antia et al.[14], to show that passive attrition is a general property of homeostasis. We extend this result to show that suppression of autoimmune disease by frequent infection is also a general property of homeostasis. Under Quantitative Predictions in the subsection Central T Memory, we model explicitly the regulatory mechanisms of the niche of cells competing for interleukin 15 (IL-15), the niche that contains central memory T cells. In the subsection following that titled The IL-7 Niche, we model the niche of cells competing for interleukin 7 (IL-7). This niche contains naive cells and $CD4^+$ memory cells. These models are calibrated for both humans and mice. Throughout we are modeling the average expected behavior, assuming well mixed populations in the niches.

Our general framework for homeostatic regulation does not consider systems that have multiple stable values for total cell number. An example of such a system would be long-lived, non-dividing cells, with number below the maximum population size of the niche. Systems such as this are not homeostatically regulated, and adding more cells to the niche has no effect on the cells already occupying it.

The mechanisms we consider include competition for cytokines and volume constraints on a structural niche. These homeostatic mechanisms keep the total number of cells relatively constant and controlled.

In general, a differential equation for the population dynamics of cells under homeostatic regulation has the form:

$$\frac{dN}{dt} = f(N)N + r_h + r_e, \tag{2.1}$$

where N is the total number of cells in the niche, all competing for the same survival factors. The dynamics of this equation are pictorially represented in Figure 2.2. The different colors of cells in Figure 2.2 represent different antigen specificities.

The homeostatic influx r_h and the pathogenic influx r_e represent influxes of new cells, from homeostatic sources and antigenic stimulation, respectively. In the absence of any antigenic stimulation it is assumed that $r_e = 0$. The influx from antigenic stimulation typically equals the product of the infection rate and the

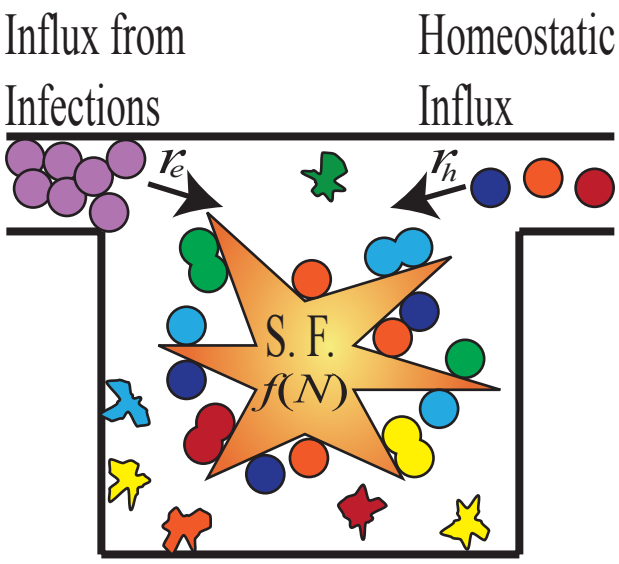

Figure 2.2: **Illustration of the dynamics of Eq. 2.1.** Cells enter the system from either infections r_e or through homeostatic influx r_h, which is zero for some niches. Survival factors (S.F.) regulate the total number of cells in the niche by either inhibiting cell death or inducing cell division. The rate of stimulation by survival factor for each cell, $f(N)$, is a function of the total number of cells in the niche, N.

number of new memory cells per infection. The homeostatic influx r_h represents new cells which arise from homeostatic sources such as thymic output. For central T memory, the niche is not likely shared with naive cells and $r_h \approx 0$, while for $CD4^+$ memory cells, there is competition with naive cells, and $r_h > 0$ [15].

The rate $f(N)$ in Eq. 2.1 gives the homeostatic regulation of death and division. $f(N)$ is called the attrition rate for reasons discussed below. This rate must be a function of the total number of cells in the niche in order for the homeostatic equilibrium to be stable. The more cells in the system the greater the level of

competition for survival, and the lower the value of $f(N)$. This gives us the requirement:

$$\frac{df}{dN} < 0. \tag{2.2}$$

The homeostatic equilibrium κ is the limiting number of cells that the system reaches when there is no antigenic stimulation, i.e. when $r_e = 0$. The homeostatic equilibrium is defined mathematically as:

$$f(\kappa) = -\frac{r_h}{\kappa}. \tag{2.3}$$

Substituting Eq. 2.3 into Eq. 2.1, along with $r_e = 0$ yields the stable ($dN/dt = 0$) solution $N = \kappa$. When $r_e > 0$ the cells generated by antigenic stimulation bring the total number above the homeostatic equilibrium, $N > \kappa$. This reduces the homeostatic renewal, such that $f(N) < -r_h/\kappa$. Except in lymphopenic conditions (where homeostatic proliferation can occur to refill the system) the attrition rate satisfies $f(N) \leq 0$.

The dynamics in Eq. 2.1 are represented pictorially in Figure 2.2. Cells enter the niche either from infections (rate r_e) or from homeostatic sources (rate r_h) and compete with each other and the cells already occupying the niche for the limited amount of survival factors. The survival factors could either act by initiating cell division or by inhibiting cell death.

2.3 Passive Attrition

After the completion of an immune response there will be a sub-population of memory cells belonging to the niche x_i. Here x_i is the number of cells of type i. The different sub-populations are unique in their antigen specificity but not in their ability to compete for survival factors. The negative value of $f(N)$ under the addition of new cells has consequences for the dynamics of these sub-populations. Since these populations share the same niche they will have the same homeostatic regulation term. However, these cells are not restimulated antigenically or added to appreciably from homeostasis, so the equation describing the time evolution of an individual sub-population lacks a source term:

$$\frac{dx_i}{dt} = f(N)x_i, \quad N = \Sigma_j x_j. \tag{2.4}$$

If there is no influx of new cells ($r_h = r_e = 0$) then $f(N) \to 0$ at equilibrium, and the individual memory cell populations are sustained indefinitely (ignoring stochastic effects, the subject of future research). With either $r_h > 0$ or $r_e > 0$, $f(N) < 0$ and the subpopulation will experience "passive attrition"[14, 16, 17], an exponential decrease in cell number over time with the rate $f(N)$, hence the term "attrition rate" for $f(N)$.

Typical memory scenarios are shown in Figure 2.3. Antigen specific cell number x_i grows rapidly over the course of a few days in response to an infection (not

modeled here). After the infection is cleared there is rapid cell death and memory formation until the total number of cells N returns to a value near κ (at the time indicated by the dashed black line). The cell populations will then experience attrition with rate $f(N)$.

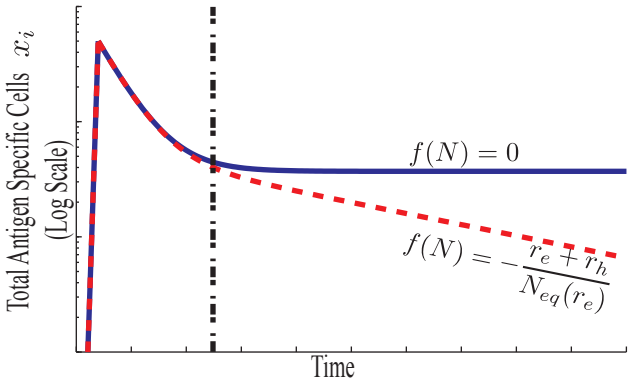

Figure 2.3: **Memory formation with and without passive attrition.** For both scenarios the number of antigen specific cells quickly rises during an immune response, then rapidly decreases until the total cell number is approximately at equilibrium, $N \approx N_{eq}$, as indicated by the black dashed line. The blue curve illustrates the case with no passive attrition, where $N_{eq} = \kappa$, and $r_e = r_h = 0$. $CD8^+$ memory in a sterile environment is representative of this (blue) scenario. The red curve illustrates the scenario where new cells are frequently added to the niche shared by the specific memory, causing the number of antigen specific cells to decline over time.

The decrease of specific memory over time is a result of infections or influx of new cells raising the total number of cells and hence the level of competition for survival factors. Central T memory in a sterile environment can survive indefinitely, as $r_e = r_h = 0$, and therefore the rate of attrition $f(\kappa) = 0$[15]. However,

for the IL-7 niche, the influx of new naive cells to the niche should contribute to the passive attrition of $CD4^+$ memory and may be responsible for the observed bi-phasic decay[15].

2.3.1 Suppression of Autoreactive Cells

We refer to sub-populations of cells that respond to either native antigen or allergen as simply autoreactive. In this case there will be an additional term (first term on the right hand side) for antigenic stimulation:

$$\frac{dx_a}{dt} = \gamma_a x_a + f(N)x_a. \tag{2.5}$$

The antigenic stimulation rate of these cells is a complicated function involving competition for antigen, tolerance mechanisms such as regulatory T cells, and physiological changes in antigen presentation from inflammation and tissue damage.

We are interested in the behavior of a very small number of cells, before disease, and specifically whether the cell population proliferates or is suppressed. The antigenic stimulation rate γ_a, is the limiting value of this more complex rate, in the low cell number limit. The antigenic stimulation rates of different clones of cells will differ. The subscript on γ_a denotes the different growth rates for the different clones, x_a.

There are two opposing rates for autoreactive cells, the rate of attrition $f(N)$ which acts to reduce their number, and antigenic stimulation γ_a which causes proliferation and eventually disease. Depending on which of these rates is larger there are two possible outcomes for populations of autoreactive cells:

$$\begin{array}{cc} \gamma_a < -f(N), & \gamma_a > -f(N). \\ \textbf{Suppression} & \textbf{Proliferation} \end{array} \tag{2.6}$$

Suppression results in exponential decay of any new population of autoreactive cells. Proliferation results initially in an exponential growth and could eventually lead to disease.

In the absence of pathogenic influx ($r_e = 0$), autoreactive cells with $\gamma_a < r_h/\kappa$ will be suppressed. Pathogenic influx decreases $f(N)$, increasing the range of γ_a that result in suppression. Figure 2.4 shows the possible scenarios for growth or decay of a small population of autoreactive cells.

The likely scenario consists of first an autoreactive cell escaping negative selection by not experiencing all self and environmental antigens as an immature cell. As this cell matures it enters the naive population where it may be stimulated by self-antigen or allergen. The antigenic stimulation causes the cell to proliferate into a small number of autoreactive memory cells. These autoreactive memory cells may still require survival factors to persist or proliferate. If this is the case, increasing the level of competition for survival factors can suppress this cell clone

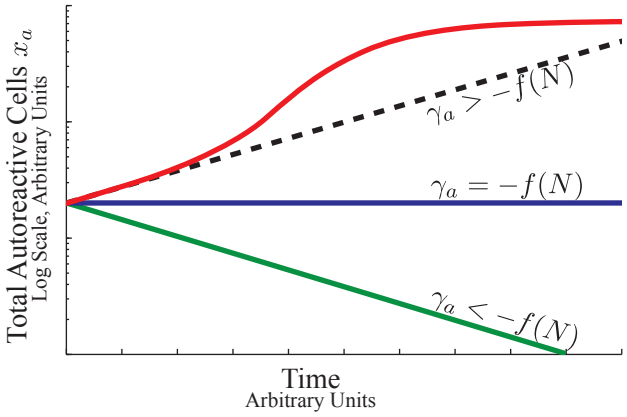

Figure 2.4: **A schematic illustration of a small population of autoreactive cells x_a.** These cells can either be suppressed if $-f(N)$ is large enough (green line) or experience exponential growth (black dashed line). If the cell population becomes large other factors will alter the growth rate such as feedbacks from inflammation and tolerance mechanisms, illustrated schematically in red.

and thereby prevent development of disease.

The suppression of autoreactive cells in this manner is accompanied by the passive attrition of memory populations. Larger values of the attrition rate $f(N)$ both suppress populations with greater ranges of antigenic stimulation rates γ_a, and causes more rapid loss of immunological memory. Conversely, for long-term stable memory populations there must be a low value of the attrition rate $f(N)$, and thus populations with a greater ranger of γ_a values will proliferate.

The inequality in Eq. 2.6 defines a boundary between suppression and proliferation that is a function of the rate of infection. Figure 2.5 illustrates a pedagogical example. The value of γ_a is a property of the cell and r_e is typically a property of

the external environment. For a clone of autoreactive cells x_a described by an antigenic stimulation rate γ_a, the boundary defines the minimum level of pathogenic influx needed to suppress that clone. For clones with large values of γ_a it is possible that there is no value of r_e large enough to suppress them. Similarly it is possible that all γ_a values below a certain limit might be suppressed by homeostatic sources of attrition, though this is not a common feature of all niches. Conversely, if we are considering an external environment that is well characterized by a particular value of r_e, the boundary in the figure defines the lower limit of autoreactivities we are likely to find in that external environment. A low r_e value corresponds to a more sterile environment while a large r_e value is associated with a "filthy" environment. In Section 2.4 we fit curves to data for human and mouse $CD4^+$ and $CD8^+$ memory cells to make quantitative predictions for these boundaries.

The Low Infection Rate Limit

We can find the asymptotic behavior of passive attrition and autoreactive suppression in the limit of infrequent infections, i.e. low r_e. The equilibrium total number of memory cells for a given rate of infections is given by $N_{eq}(r_e)$. This is simply the value of N for which the right hand side of Eq. 2.1 is equal to zero:

$$f(N_{eq}(r_e)) = -\frac{r_e + r_h}{N_{eq}(r_e)}. \tag{2.7}$$

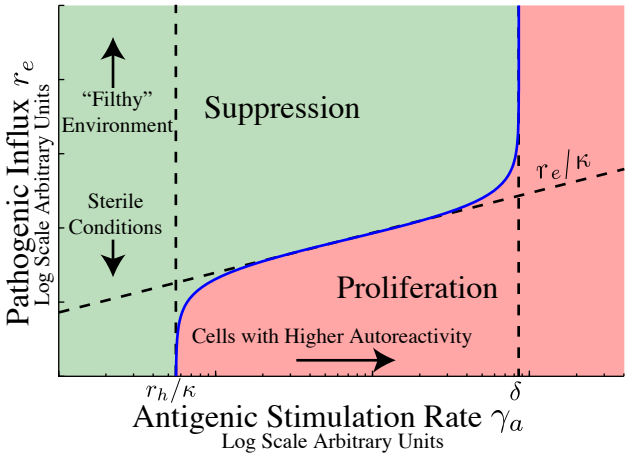

Figure 2.5: **Illustration of a boundary defined by Eq. 2.6 separating conditions for suppression (green region) and proliferation (pink region) of autoreactive cells.** The vertical axis is the pathogenic influx r_e. This quantity is typically controlled by the external environment and is expected to be proportional to the infection rate. The lower portion of the figure represents cells in a more sterile environment and the upper portion of the figure a filthy one with frequent infections. The horizontal axis is the antigenic stimulation rate γ_a for a small population of autoreactive cells x_a. Cells with antigenic stimulation rate less than r_h/κ are always suppressed, though for some niches $r_h = 0$. No populations with $\gamma_a > \delta$ (where δ is the apoptotic rate under high levels of competition for survival factor) can be suppressed by passive attrition because the division rates of these cells (from autoantigen exposure) are large enough to maintain the population even in the absence of survival factors.

If the infection rate is zero then $N_{eq}(r_e) = \kappa$, the homeostatic equilibrium. If we consider the case where the infection rate is small enough that the correction to $N_{eq}(r_e)$ is insignificant compared to κ we have $N_{eq}(r_e) \approx \kappa$. In this limit, Eq. 2.7 reduces to the form derived by Antia et. al[14]:

$$f(N_{eq}(r_e)) = -\frac{r_e + r_h}{\kappa}. \tag{2.8}$$

This gives an exponential rate of decay of existing memory populations that is proportional to the sum of the rates of new cell incorporation:

$$x_i(t) \approx x_i(0)e^{-(r_e+r_h)t/\kappa}. \tag{2.9}$$

We also have the condition for suppression in the limit of low pathogenic influx r_e:

$$\gamma_a < \frac{r_e + r_h}{\kappa}. \tag{2.10}$$

As can be seen from this equation, clones with $\gamma_a < r_h/\kappa$ are always suppressed (since $r_e > 0$).

For central memory T cells the homeostatic influx r_h equals zero, and there is no lower limit on ability of autoreactive cells to proliferate in sterile conditions. The asymptotic behavior of the boundry separating the regions of suppression and proliferation therefore follows approximately the curve r_e/κ then converges to the vertical line of r_h/κ. This asymptotic behavior can be seen in Figure 2.5 for the lower antigenic stimulation rate γ_a.

The asymptotic result shows that addition of new cells to a homeostatic niche is a mechanism for suppressing or eliminating autoreactive cells with low antigenic stimulation rate γ_a, and that it is a common feature of homeostatic regulation. For larger values of γ_a it may not be possible to satisfy Eq. 2.6. This is shown and discussed in Section 2.4 where we model the homeostasis of cells in the IL-

15 regulated niche (central memory T cells), and cells in the IL-7 niche ($CD4^+$ and naive cells) respectively. There we also give quantitative predictions for the range of antigenic stimulation rates γ_a that will be suppressed in environments characterized by the rate of pathogenic influx r_e.

2.4 Quantitative Predictions

2.4.1 Central T Memory

The best understood homeostatic regulation scheme in the mouse and human immune systems are the $CD8^+$ central memory T cell pools [18]. These cells are differentiated from effector memory by the presence of high levels of CD122 on the cell surface. The CD122 protein is part of a receptor for IL-15. In the absence of IL-15 the central memory T cells can not survive. Other cell types are typically unaffected in the IL-15 knockout mouse [19] showing that the niche is not shared and that competition between the cells of this niche for IL-15 should have little effect on other cell types. Additionally we know that in a sterile environment memory populations in this niche are stable yielding $r_h = 0$ [20].

At homeostatic equilibrium the total number of cells remains constant. Since there is no homeostatic influx of new cells to this pool ($r_h = 0$), both the homeostatic division rate α_h and the homeostatic death rate δ_h are therefore equal. With

CSFE staining and other techniques it has been observed for mice that the homeostatic division rate is approximately once every 2-3 weeks, meaning $\alpha_h = \delta_h =$ (2-3 weeks)$^{-1}$ [21].

To discern whether IL-15 inhibits apoptosis or stimulates division, we consider the two possible cases separately. Inhibition of apoptosis is described by:

$$\frac{dN}{dt} = \alpha_h N - \delta(L)N, \tag{2.11}$$

where N is the population size, the first term on the right hand side represents increases in the population due to division , and the second term represents decreases due to apoptosis. The quantity L is the concentration of IL-15 and the apoptotic rate $\delta(L)$ decreases with increasing L. Judge et al. [19] placed central memory T cells in an IL-15 saturated solution. In the saturated environment we would expect $\delta(L) = 0$, and if Eq. 2.11 were the correct description we would see the proliferation rate of the population equal to $\alpha_h =$ (2-3 weeks)$^{-1}$. Instead the population was observed to double in less than three days which rules out Eq. 2.11 as a valid model. From this we conclude that IL-15 does not simply inhibit apoptosis.

Next we consider the stimulation of division by IL-15, described by the equation:

$$\frac{dN}{dt} = \alpha(L)N - \delta_h N. \tag{2.12}$$

Now the division rate $\alpha(L)$ is a function of IL-15 concentration L, and increases with increasing L. Another experiment by Judge et al.[19] transplanted central memory T cells into IL-15 knockout mice. In the absence of IL-15 and stimulating antigen, $\alpha(0) = 0$, Eq 2.12 predicts a decay in cell number with rate $\delta_h =$ (2-3 weeks)$^{-1}$. The observed decay took place over approximately 2 weeks [19] in agreement with the model. This implies that to a first approximation IL-15 stimulates division.

We can compare the homeostasis expressed in Eq. 2.12 with our general model of suppression to obtain asymptotic behavior of the boundary separating suppression from proliferation, described by Eq. 2.6. Our previous requirement that $f(N)$ be a decreasing function of N, requires that $\alpha(N)$ also be everywhere decreasing. Physically, this corresponds to the concentration of L being lower the more cells there are competing for it. This gives us (from Eq. 2.6) the conditions for suppression:

$$\gamma_a < \delta_h - \alpha(N), \quad \text{with} \quad \frac{d\alpha}{dN} < 0. \tag{2.13}$$

There can therefore be no suppression by passive attrition for cells with $\gamma_a > \delta_h$. Physically, this corresponds to cells that can sustain their number through antigenic stimulation alone (characterized by large γ_a) and do not require homeostatic signals for survival. The condition for suppression of autoreactive cells, as $\gamma_a \to \delta_h$, requires that $r_e \to \infty$. This asymptote is drawn explicitly in Figure 2.5 and is

evident in the plots of Fig. 2.6.

The asymptotic behavior for the condition of suppression of autoimmune disease by passive attrition is given by only two parameters, κ the homeostatic equilibrium number of cells in the niche, and δ_h the homeostatic division rate of the population. Connecting the low r_e behavior, Eq. 2.10, with the behavior as $\gamma_a \to \delta_h$ requires a more detailed model of the competition for IL-15.

Biologically, IL-15 is typically presented to central memory T cells by dendritic cells. The IL-15Rα receptor on dendritic cells binds to IL-15 and presents it to the central memory cells where it binds to the CD122 molecule initiating signaling.

A rate equation that captures the correct asymptotic behavior in both limits and has an interpretation relating to competition for growth factor is a saturating function:

$$\alpha(N) = \frac{1}{\omega_0 + \omega_1 N}. \tag{2.14}$$

This rate equation has the physical interpretation that the inverse of the rate, α^{-1}, is the expected waiting time for stimulated division, and the waiting time is a linear function of N. The shortest possible physiological waiting time is given by ω_0, and in a system with more cells, the waiting time increases linearly as the competition for growth factor among cells increases. (The denominator in Eq. 2.14 can be viewed as the first order approximation of a more complicated function of waiting time $\omega(N)$.)

Inserting this into the population dynamics equation (Eq. 2.1 with $r_h = 0$) yields the homeostatic equation:

$$\frac{dN}{dt} = \frac{N}{\omega_0 + \omega_1 N} - \delta_h N + r_e. \tag{2.15}$$

This equation is functionally equivalent to the equation used by Utzny and Burroughs [22]. The homeostatic equilibrium ($dN/dt = 0, r_e = 0$) value κ is given by:

$$\kappa = \frac{1}{\omega_1}\left(\frac{1}{\delta_h} - \omega_0\right), \tag{2.16}$$

and the equilibrium total number of memory cells in the presence of infections, $N_{eq}(r_e)$ is given by:

$$N_{eq}(r_e) = \left(\kappa + \frac{r_e}{\delta_h}\right)\left[\frac{1}{2} + \frac{1}{2}\sqrt{1 + \frac{4\frac{\omega_0}{\omega_1}\frac{r_e}{\delta_h}}{\left(\kappa + \frac{r_e}{\delta_h}\right)^2}}\right] \tag{2.17}$$

$$\approx \kappa + \frac{r_e}{\delta_h}. \tag{2.18}$$

The approximate form is valid when the expected lifetime of a cell is much larger than the shortest time to division: $\delta_h^{-1} \gg \omega_0$. Experimentally δ_h^{-1} is on the order of weeks while ω_0 is approximately a day. The approximation is therefore a good one.

This gives us a functional form for the condition for suppression of autoreactive populations:

$$\gamma_a < \frac{r_e}{N_{eq}(r_e)} \approx \frac{r_e}{\kappa + \frac{r_e}{\delta_h}}. \tag{2.19}$$

This relation for autoreactive suppression by passive attrition relies on just two parameters: the homeostatic equilibrium κ, and the homeostatic death rate δ_h. The right hand side of Eq. 2.19 is equal to the attrition rate $f(N)$ of the various memory populations in the niche, not being re-stimulated. This provides an observable quantity to test the model.

The conditions for suppression of autoreactive cells with stimulation rate γ_a, with respect to new memory incorporation r_e, is plotted in Figure 2.6 for humans (solid lines) and mice (dashed lines). The parameter values for central T memory are found in Table 2.1. If the initial growth rate of an autoimmune disease is measured, these charts will tell if the autoreactive population can be suppressed, and if so, what rate of new central memory incorporation is required. Alternatively, if an environment is characterized by measuring passive attrition rates, this chart will show what autoreactivities will be suppressed by those environmental conditions.

2.4.2 The IL-7 Niche

The niche for $CD4^+$ T cells is more complex than that for central T memory. The Th1 and Th2 $CD4^+$ memory cells share their niche with naive $CD4^+$ and naive $CD8^+$ cells. While cells in this niche may require both IL-7 and MHC contact, competition for MHC contact is not likely a limiting factor in homeostatic survival

Parameter Values							
Parameter	Units	Human			Mouse		
		IL-15	IL-7	Refs	IL-15	IL-7	Refs
δ_h	day^{-1}	1/102	1/68	[20]	1/17	1/10	[21]
κ	cells	25×10^9	268×10^9	[23] [20]	9×10^6	7.6×10^7	[20]
r_h	cells/day	0	1.7×10^8	[15] [20]	0	7.3×10^4	[20]

Table 2.1: Numerical values for memory cells in mice and humans. The values of κ for IL-7 are the sum of naive and memory CD4$^+$ and naive CD8$^+$ cells. For humans the fraction of cell types in the blood was taken from Vrisekoop [20] and extrapolated to the total body using total cell numbers from Ganusov [23]. For mice, cell numbers in the spleen were taken from Vrisekoop [20] and extrapolated to whole body based on estimates of 3×10^7 naive CD8 T cells in the whole body. The r_h value for mice is taken from measurements of specific memory attrition, while for humans it is estimated from thymic output. Because we are interested in attrition rates the indirect measure provides better modeling accuracy.

due to its ubiquity.

Assuming that the action of IL-7 is similar to that of IL-15 we have an equation similar to Eq. 2.15, but with an additional term for homeostatic influx of cells entering the niche from the thymus, r_h:

$$\frac{dN}{dt} = \frac{N}{\omega_0 + \omega_1 N} - \delta_h N + r_e + r_h. \tag{2.20}$$

The values of κ, ω_0, ω_1, and δ_h are different for the cells belonging to the niche competing for IL-7, than they were for central memory T cells. In this niche the total number of cells at homeostatic equilibrium κ, is the sum of the number of CD4$^+$ memory, CD4$^+$ naive, and CD8$^+$ naive cells at homeostatic equilibrium, since they are all competing for IL-7.

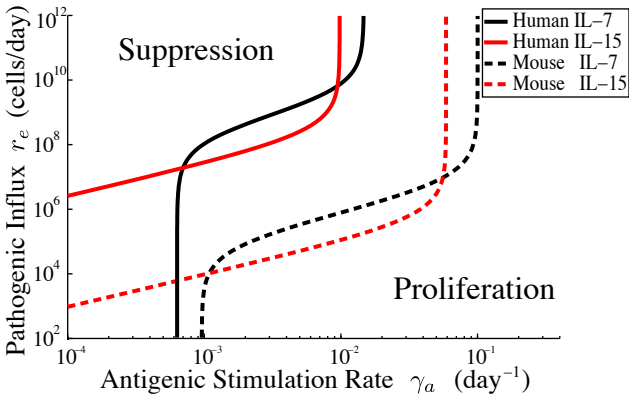

Figure 2.6: **Boundaries discriminating between autoreactive cell populations that are suppressed vs. those which proliferate, for humans (solid lines) and mice (dashed lines).** The condition for suppression is given by Eq. 2.19 and 2.25 and the numerical values of the parameters are found in Table 2.1. The features of these curves are discussed in the caption to Fig. 2.5. Central T memory cells belong to the IL-15 niche (red lines). The model predicts that for CD4$^+$ T cells which are in the IL-7 niche (black lines), all autoreactive populations x_a with antigenic stimulation rates γ_a below r_h/κ are suppressed by the homeostatic influx of naive cells. Passive attrition can not suppress autoreactive cells with $\gamma_a > \delta_h$.

The rate of homeostatic homeostatic influx r_h leads to passive attrition of CD4$^+$ memory cell populations, even in sterile conditions. For mice the rate of attrition of CD4$^+$ memory populations in a controlled environment has been measured to be around $-f(\kappa)$ =(450 days)$^{-1}$ [15]. We know from Eq. 2.1 and 2.4, that the rate of attrition in the absence of pathogenic influx r_e is given by $-f(\kappa) = r_h/\kappa$, so:

$$r_h = -f(\kappa)\kappa. \tag{2.21}$$

The numerical values for mice and humans are presented in Table 2.1. For humans

the value of r_h is taken from the thymic output of patients in their early 20s [20].

The formula for the homeostatic equilibrium κ in the IL-7 niche is more complicated than for central memory due to the homeostatic influx r_h. The total number of cells based on the parameters of the model is:

$$\kappa = \left[\frac{1}{\delta_h\omega_1} - \frac{\omega_o}{\omega_1} + \frac{r_h}{\delta_h}\right]\left[\frac{1}{2} + \frac{1}{2}\sqrt{1 + \frac{4\frac{\omega_0}{\omega_1}\frac{r_h}{\delta_h}}{\left[\frac{1}{\delta_h\omega_1} - \frac{\omega_o}{\omega_1} + \frac{r_h}{\delta_h}\right]^2}}\right] \tag{2.22}$$

$$\approx \frac{1}{\delta_h\omega_1} - \frac{\omega_o}{\omega_1} + \frac{r_h}{\delta_h}, \tag{2.23}$$

where the approximate form is valid if the expected life time is greater than the fastest possible time to division, $\delta_h^{-1} \gg \omega_0$. These two terms are observed to be approximately 10 days[21] and 12 hours, respectively[22].

We also have the form for the expected number of cells in the niche when the pathogenic influx r_e is non-zero:

$$N_{eq}(r_e) \approx \kappa + \frac{r_e}{\delta_h}. \tag{2.24}$$

This gives us the conditions for the suppression of autoreactive $CD4^+$ memory. From Eq. 2.1:

$$\gamma_a < \frac{r_e + r_h}{\kappa + \frac{r_e}{\delta_h}}. \tag{2.25}$$

Figure 2.6 shows the values of γ_a that are suppressed at a range of r_e values for for $CD4^+$ T cells (black curves) for both humans (solid curve) and mice (dashed curve).

There are two additional effects which arise from the shared niche between the naive and Th1 and Th2 memory populations: the attrition of naive populations by inclusion of new memory, and a uniform suppressive effect, rather than a delicate balance of the Th1/Th2 ratio. The delicate balance for Th1/Th2 ratio is another proposed mechanism to explain the hygiene hypothesis.

The naive population typically contains many clones of small number. In a niche shared with memory cells, naive cells experience passive attrition. This results in the elimination of some naive sub-populations. This thinning of the naive repertoire has previously been studied [14, 24], is a major contribution to immunosenescence and is studied in detail in Chapter 3. The separation of the memory and naive niches, as in the case of $CD8^+$ cells, prevents this effect.

We have assumed here that the action of IL-7 stimulates division in the same was as IL-15. This assumption is based on the similarity and commonality between the receptor molecules for both interleukins. However, if IL-7 acts by inhibiting apoptosis, the boundary between suppression and proliferation (Eq. 2.19 and 2.25 and Fig. 2.5 and 2.6) will have the same low γ_a behavior but will have a vertical asymptote at the faster rate δ_m, the rate of cell death in the absence of IL-7.

2.5 Experimental Predictions

We have shown the conditions for suppression of immune system disorders by passive attrition for central memory $CD8^+$ and (under the assumption that IL-7 has an effect similar to IL-15) $CD4^+$ memory. We have also shown that this mechanism is not unique to these cell types but that it applies to any cell type under homeostatic regulation.

Autoreactive cells with $\gamma_a > \delta_h$ (right hand side of Figure 2.6) would receive antigenic stimulation at a rate rapid enough to maintain the population in the absence of homeostatic survival factors. Passive attrition would not be able to suppress these cells for this reason. Presumably, these cells are removed by negative selection as they are the most autoreactive, and if they were not removed autoimmune disease would be much more common. Negative selection provides tolerance to autoimmune diseases by removing the most autoreactive lymphocytes before they mature. If all cells with autoreactivity above a threshold value γ_c are removed by negative selection, this model would tell us the influx of new memory (i.e. infection rate) required to suppress all autoreactivities less than γ_c, the autoreactive cells that may escape negative selection. In this manner the two tolerizing mechanisms in combination can cover the entire spectrum of γ_a values.

This quantitative model makes experimentally testable predictions. We pro-

pose the following experiment illustrated in Figure 2.7. Experimental Protocol:

1. Create an antigen specific memory population. This will be used for a direct measurement of the attrition rate $f(N)$.

2. Active transfer of a small population of autoreactive cells. This population should be large enough to induce autoimmune disease in an animal in a sterile environment.

3. Time-series of new memory inclusions. Active transfer of non-autoreactive memory cells, not specific for the antigen used in Step 1, or induction of new memory cells to create a range of r_e values.

4. Repeated measurements during time-series of new memory inclusions. Count how many of the initial specific memory population x_i are present, to measure the attrition rates. Count the autoreactive cell number x_a. In the case of $r_e = 0$ the measurement of autoreactive cell number will allow calculation of γ_a for that autoreactive clone.

5. Examine animals for pathology of transfered autoimmune disease.

Measuring the passive attrition rate by a time series count of the specific memory population created in step 1 will eliminate any uncertainties associated with the active transfer process. Inducing passive attrition through infection or immuniza-

tion could also complicate the experiment by activating other inflammatory and tolerizing aspects of the immune response. It would be best therefore, to first perform the experiment with active transfer of memory cells in Step 3 to eliminate the possibility of these complications.

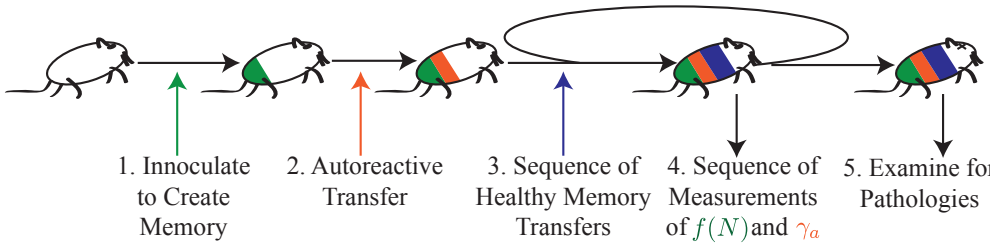

Figure 2.7: **Schematic of proposed experimental protocol.** Individual steps 1-5 are described in more detail in the corresponding enumerated list in the text.

Active transfer of memory cells eliminates other possible suppressive mechanisms. Performing the above experiment using infections will show the extent to which other mechanisms may suppresses autoimmune disease through pathogenic infection. Similar results for the active transfer and infection experiments would indicate that passive attrition is the dominant mechanism in nature for suppression of immune disorders by pathogen.

Measuring passive attrition rates presents a method of characterizing an environment. Though performing the above experiment for humans may be difficult, looking at regional trends in passive attrition rates and comparing them with prevalence of autoimmune disorders should yield an anti-correlation between the

two quantities. The passive attrition rates in humans in different regions could most easily be measured by looking at the numbers of cells specific to smallpox vaccines, as this sub-population of cells is not likely to have been re-stimulated. The attrition rates of smallpox immunity have been measured for vaccinia virus [25]. To our knowledge a regional study has not been performed.

It has also been suggested that the beneficial effects of exposure to infectious diseases are most important for children [2]. There are two effects that may contribute to this: the expansion of the niche may favor autoreactive growth, and the higher flux of new cells from the thymus increases the rate of new autoreactive cells entering the niche. Mathematical modeling of the effects of passive attrition on autoreactive populations under these conditions is the subject of current work.

The competition for survival factors (i.e. passive attrition) is one of several proposed mechanisms by which infectious diseases may confer protection from immune system disorders. Other proposed mechanisms include Th1/Th2 balance, and generation or activation of regulatory T cells by infection.

Th1 and Th2 cells each have a suppressive effect on the other. A system out of balance in population numbers might result in one cell type being unregulated by the other. Th1 cells are implicated in autoimmune diseases while Th2 cells are a component of allergic disease. If Th1/Th2 balance is the mechanism generating a suppression of immune system disorders, we expect allergy and autoimmune

prevalence to be inversely correlated. However, this is not the case[2]. It has also been observed that individuals with diabetes or rheumatoid arthritis have a higher incidence of atopic disease [2, 11, 10], in contradiction to the hypothesized Th1/Th2 balance dynamic. This observation is in agreement with the predictions of passive attrition. Suppression by passive attrition is independent of the method of new cell introduction, whether it is from a Th1 or a Th2 response. It only depends on the number of new cells created that are competing for IL-7.

Bystander suppression by regulatory T cells in response to infections is a compelling hypothesis. These cells have many possible mechanisms of suppression, and characterization of these cell types is still in its infancy. It has been shown that the suppressive effects conferred by killed bacteria persist in IL-10 and IL-4 knockout NOD mice [2, 12]. These suppressive cytokines however are only two of the several possible mechanisms that regulatory T cells may be using to suppress immune system disorders so this mechanism can not currently be ruled out.

Mathematical models of the expected level of protection conferred by each of these mechanisms will give rise to insight testable predictions that will reveal which mechanisms are dominant. Passive attrition should be capable of suppressing small populations of autoreactive cells, but it comes with the price of accelerated loss of immunity. This tradeoff is one of many the immune system must balance.

Chapter 3

Robustness and Fragility in Immunosenescence

This chapter develops a model of the adaptive immune response. It looks at what immunity means and how it is acquired. It then looks at the effects of immunity acquisition over a life time in a niche shared by both naive and memory cells. This could be the IL-7 niche discussed in the previous chapter or possibly the B-cell niche which little is known about. This long term memory acquisition causes attrition of the naive cells in the niche. We use an approximate form of the homeostasis model discussed in the previous chapter, keeping the total number of cells in the niche constant over long times, and see a shift from a naive dominated niche in adolescence to a memory dominated niche in the elderly. The constraint

on the number of cells implies that memory, which is specific to infections the system has seen, comes at a price for unseen infections [26]. This illustrates how the immune system initially increases in effectiveness but eventually becomes overspecialized with age. This has correspondence with a class of complex systems referred to as "Robust yet Fragile." This chapter also introduces the modeling of the diversity of the lymphocyte repertoire.

3.1 The Adaptive Immune System

The adaptive immune system [27] of vertebrates has evolved in a manner which enables adaptation to the history of infections over the lifetime of each individual organism. It consists of a complex, heterogeneous collection of cells that is derived from stem cells in the bone marrow, and proliferates in the lymph nodes. These cells are endowed with the remarkable ability to discriminate between self and non-self agents within the body and remove the non-self elements [28, 29, 30]. B and T cells are the white blood cells (i.e. lymphocytes) that constitute the adaptive components of the immune system. They derive their ability to discriminate self from non-self with the binding specificity of their receptors: T cell receptors for T cells, and membrane bound antibody for B cells. These receptors are assembled randomly from gene segments, producing a population of naive cells, in which

each individual combination has a different binding specificity (VDJ recombination). The random combinations of genes gives the immune system the ability to produce diverse cells capable of responding to many pathogens. During an infection, the cells whose receptors recognize the antigen proliferate and differentiate into antigen removing effector cells and long-lived memory cells. The memory cells give rise to a more rapid and efficient response to a secondary exposure to the same antigen. However, due to homeostatic regulation of the lymphocyte population, the growth of memory cells reduces the naive cell population size. Over time, this has the effect of increasing sensitivity to novel infections.

The process in this chapter can be broken down into three stages on differing time scales: (i) antigen proliferation and immune response in an individual infection, (ii) recovery and stasis between infections, (iii) long term adaptation of lymphocyte populations over the lifetime of the individual. We assume that rates of infection are small enough that the immune system completely eliminates one pathogen, and relaxes to the uninfected state long before the next infection occurs. This allows us to introduce our model in three stages, corresponding to the increasing time scales (i)-(iii) above, beginning with an individual infection.

3.2 Model of Immune Response

The immune response model consists of coupled differential equations for immune system cell populations, defined in terms of their primary immunological function and their binding characteristics. The relative population sizes evolve in time, stimulated by episodic infections. Antigens are drawn from a probability distribution on their characteristics, which enables estimation of the binding affinity of lymphocytes. We include a constraint on the total number of immune cells in the system, and define an immunological loss function that quantifies disease severity.

Characteristics of the distinct populations in our model are summarized in Table I. Note that in our simplified model, as in Segel and Pereleson [30], lymphocytes (memory, naive and effector cells) are not specifically T or B cells, but a generalization having properties common to both types. We have also omitted helper T cells (that help to stimulate the immune response), as well as the complex germinal center reaction and somatic hypermutation (processes involving the proliferation and development of lymphocytes), assuming these features are not limiting factors in immunosenescence.

Species	Symbol	Primary Function
Antigen	$A(\vec{x}, t)$	Chemical that stimulates an immune response, which acts to remove it from the body.
Effector	$E(\vec{y}, t)$	Short lived cells that remove antigen from the body.
Naive	$N(\vec{y}, t)$	Short lived detector cells generated in the bone marrow with randomly assembled receptors. When stimulated these divide into memory and effector cells.
Memory	$M(\vec{y}, t)$	Long lived detector cells having exactly the same receptor as the parent. Like naive cells, when stimulated these also divide into more memory and effector cells.
Dendritic	$F(t)$ and $F^*(t)$	Antigen presenting cells which act as catalysts. F traps antigen, converting to F^*. F^* facilitates the stimulation of naive and memory cells, which converts it back to F.

Table 3.1: Immune system model ingredients. Population sizes are functions of time t, and evolve as defined below. Aside from the dendritic cells, all populations have binding characteristics represented as vectors in an abstract shape space. Increasing proximity between an antigen and effector corresponds to increasing effacacy of the immune response.

Shape Space

In our model, A, E, N, and M are all fields on a generalized shape space, introduced by Oster and Perelson [31] to represent the lock-and-key type specificity of antigen-receptor binding. The dimensions of the generalized Euclidean shape space correspond to quantities such as size, charge distribution, and hydrophobicity. This differs from other Hamming type shape space models where each dimension pertains to a particular amino acid in the binding region sequence [32]. The binding sites on the antigens and receptor proteins are described by the position vectors in the shape space, $\vec{x}$ and $\vec{y}$, respectively. The binding of antigen to dendritic cells as described in Table I, is not shape space dependent. All antigens in this model bind to dendritic cells with the same affinity. Recent calculations indicate that the shape space is best described with between five and eight dimensions [32]. We use two dimensions here for visualization. Using higher dimensions in the model changes the distribution of affinities, but does not dramatically effect the results of the chapter. Extensions to higher dimensions, as well as the more complex interactions listed above, will be considered in future work.

Vector values of the antigen $\vec{x}$ and immune cells $\vec{y}$ describe complementary binding characteristics, so that the binding affinity for $A(\vec{x})$ and a receptor at $\vec{y}$,

given by $\gamma(\vec{x}, \vec{y})$, is maximal for $\vec{x} = \vec{y}$. For $\vec{x} \neq \vec{y}$ the binding affinity is a decaying function of the distance from $\vec{x}$ to $\vec{y}$ in the shape space $\gamma = \gamma(|\vec{x} - \vec{y}|)$. Following Segel and Pereleson [30], we take the affinity function to be a Gaussian:

$$\gamma(\vec{x}, \vec{y}) = \gamma_{max} e^{-(\vec{x}-\vec{y})^2/(2b^2)}, \tag{3.1}$$

where γ_{max} sets the overall scale for the strength of the immune response, and b sets the mismatch tolerance between antigens and receptors. Replacing γ with different decaying functions of distance (e.g. exponential) does not significantly alter the results of this work.

Periods of infection are associated with introduction of antigen. Different diseases are associated with different shape space coordinates $\vec{x}$, and have different rates of infection. Upon infection, a pathogen proliferates at an exponential rate so that the antigen population grows at a rate $\beta A(\vec{x})$ (Eq. (2)). In our model, $t = 0$ marks the time when the pathogen is mixed into the lymph and begins to stimulate an immune response. We assume a finite value of $\mathrm{A}(\vec{x}, 0)$ at this onset to account for the delay in the start of the immune response. This represents how once a small amount of the pathogen bypasses the physical barriers of the innate immune system it will proliferate until it finds its way into the blood and then lymph nodes, at which point the immune response is triggered.

Next the unoccupied dendritic cells, F, begin to trap antigen and become

activated to F^* at a rate $\rho F A(\vec{x})$ (Eqs. (2-3)). The activated dendritic cells F^* now present antigen to the naive and memory cells stimulating them to divide (Eqs. (3-5)). Overall, the stimulation occurs at a rate $\alpha\gamma(\vec{x},\vec{y})F^*(N+M)(\vec{y})$. Here the factor of $\gamma(\vec{x},\vec{y})$ gives the highest affinity lymphocytes the most rapid stimulation. The daughters of the cellular division of either $N(\vec{y})$ or $M(\vec{y})$, are $E(\vec{y})$ cells with fraction f, or $M(\vec{y})$ cells with fraction (1-f) (Eqs. (4-6)). Several generations of memory cells may therefore be produced through an immune response. In stimulating naive and memory cells F^* reverts back to F (Eq. (3)) keeping the total $F + F^* = H$ constant. This rate is the integral of the rate of N and M stimulation over the entire shape space. Effector cells eliminate antigen from the system with rate $A(\vec{x})\gamma(\vec{x},\vec{y})E(\vec{y})$. The total rate of antigen removal is the integral of this rate over the shape space of effector cells (Eq. (2)). Effector cells are short lived and die with rate $\delta E(\vec{y})$ (Eq. (6)).

These short time scale reactions are described by the following system of equa-

tions (we drop the explicit t dependence in all populations to simplify notation):

$$\frac{\partial A(\vec{x})}{\partial t} = \beta A(\vec{x}) - A(\vec{x}) \int \gamma(\vec{x},\vec{y}) E(\vec{y}) d\vec{y} - \rho F A(\vec{x}) \tag{3.2}$$

$$\frac{\partial F^*}{\partial t} = \rho F A(\vec{x}) - \alpha \int \gamma(\vec{x},\vec{y}) F^* (M+N)(\vec{y}) d\vec{y} \tag{3.3}$$

$$\frac{\partial N(\vec{y})}{\partial t} = -\alpha \gamma(\vec{x},\vec{y}) F^* N(\vec{y}) \tag{3.4}$$

$$\frac{\partial M(\vec{y})}{\partial t} = (2-2f)\alpha\gamma(\vec{x},\vec{y}) F^* N(\vec{y}) + (1-2f)\alpha\gamma(\vec{x},\vec{y}) F^* M(\vec{y}) \tag{3.5}$$

$$\frac{\partial E(\vec{y})}{\partial t} = 2f\alpha\gamma(\vec{x},\vec{y}) F^* (M+N)(\vec{y}) - \delta E(\vec{y}) \tag{3.6}$$

Here α is an affinity independent factor that accounts for the difference in $\gamma(\vec{x},\vec{y})$ dependent rates of lymphocyte stimulation and removal of antigen. Note that our model does not include any spatial variables for position of antigen and lymphocytes in the body, which corresponds to assuming a well mixed system. This system of equations exhibits many features we expect from an immune system model, such as rapid secondary response and affinity selection.

During the immune response the naive and memory cells are indistinguishable. In our model their difference becomes apparent on intermediate time scales. Therefore, we consider their combined effect using a single variable $D(\vec{y}) = N(\vec{y}) + M(\vec{y})$. Figure 3.1 shows a typical response to a repeated inoculation with antigen $\vec{x}$. Although other lymphocytes also bind less effectively to the antigen, for illustrative purposes we plot only populations $E(\vec{y})$ and $D(\vec{y})$ for $\vec{x} = \vec{y}$,

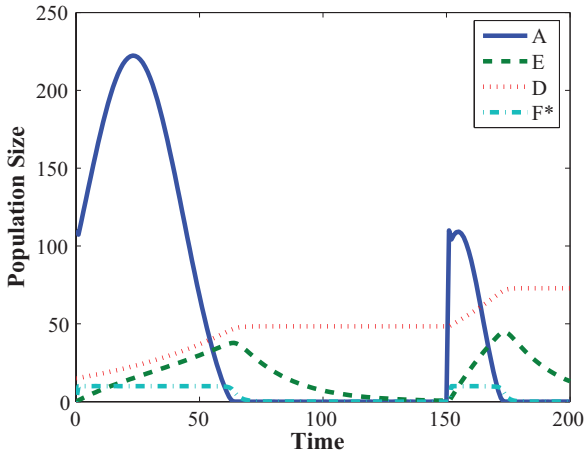

Figure 3.1: Immune responses to two sequential inoculations by the same antigen. Results are shown for maximum binding affinity pairs $\vec{x} = \vec{y}$. The rapid response to the secondary inoculation (represented by the smaller size of the second peak) is due to the elevated number of memory cells. The immunological loss Eq. (3.15) is defined to be the area under the antigen population peak. For the primary and secondary peaks the values are 8,860 and 1,525, respectively. The model parameters used in this and all simulations in this chapter are as follows: $\alpha = 1.5, \beta = 0.083, f = 0.38, \delta = 0.01, \rho = 1, \phi = 10^{-4}, H = 10, \gamma_{max} = 0.005, b = 2$. These parameter values give typical behavior for the model.

as well as F^* (for which binding is independent of shape space characteristics).

Initially there are 15 memory cells with $\vec{x} = \vec{y}$, $D(\vec{y}, 0) = 15\delta(\vec{x} - \vec{y})$, $F = H$, $E = 0$, and an antigen inoculation $A(\vec{x}, 0)$=110. After the first immune response is complete, there is a second identical inoculation at a later time. In each exposure, the population size of the antigen increases, until a sufficient number of effector cells are created from the memory and naive cell populations to eliminate the infection. The total number of lymphocytes $N + M + E$, increases during an

immune response, corresponding to swelling of the lymph nodes. As the effectors die and the memory and naive cells are no longer stimulated, the swelling subsides. Additionally, this model predicts that symptoms associated with elevated E levels peak just as the pathogen is cleared. The more rapid secondary response is due to the elevated number of memory cells. (The initial steep decline in the secondary response is due to the trapping of antigen by the dendritic cells.) All other model parameters remain the same from the first exposure to the second. Between infections all short lived effector cells die, and the F^* cells all revert to F.

To quantify the severity of an individual infection we define a loss function $L(\vec{x})$ as the integral of the antigen population size with respect to time:

$$L(\vec{x}) = \int A(\vec{x}, t)dt. \tag{3.7}$$

While physiologically severity of disease depends on many factors, we believe that this is a simple natural choice, as it is a rough measure of the amount of the body's resources a pathogen may consume and the amount of toxin the pathogen may secrete. This immunological loss function serves as a tool for quantifying statistics of infection size, and provides a meaningful target for sensitivity analysis. In the context of this investigation and immunosenescence, it allows us to quantify fitness and monitor how it changes over the development of the immune system. Additionally, loss can be used to compare the effects of additional immune sys-

tem components and reactions in more detailed immune system models, and to quantify the efficacy of drugs and therapies based on their effect on loss.

We can obtain analytic estimates for loss as well as memory cell population growth as functions of pre-infection memory and naive cell population sizes based on several simplifying approximations to Eqs. (3.2-3.6). For $\rho A \gg \alpha\gamma$, F^* is approximately equal to the total number of dendritic cells H, $F^* \approx H$ and $F \approx 0$. Since A levels will be high when an immune response is initiated this approximation is reasonable. Equations (3.2-3.6) with M and N replaced with $D = M + N$, and the approximation $F^* \approx H$, reduce to:

$$\frac{\partial A(\vec{x})}{\partial t} = \beta A(\vec{x}) - A(\vec{x}) \int \gamma(\vec{x},\vec{y}) E(\vec{y}) d\vec{y}, \tag{3.8}$$

$$\frac{\partial E(\vec{y})}{\partial t} = 2f\alpha\gamma(\vec{x},\vec{y}) H D(\vec{y}) - \delta E(\vec{y}), \tag{3.9}$$

$$\frac{\partial D(\vec{y})}{\partial t} = (1-2f)\alpha\gamma(\vec{x},\vec{y}) H D(\vec{y}). \tag{3.10}$$

These equations can be easily integrated yielding solutions which approximate the antigen population size during an infection. The complete expression for $A(\vec{x},t)$ is tractable, but cumbersome, and takes the form

$$A(\vec{x},t) = A(\vec{x},0) e^{\beta t - \int d\vec{y} S(\vec{x},\vec{y},t)}. \tag{3.11}$$

A simple expansion of the function $S(\vec{x},\vec{y},t)$ to second order in t yields a Gaussian approximation for the $A(\vec{x},t)$ peaks (e.g., in Fig. 1):

$$A(\vec{x},t) = A(\vec{x},0) e^{\beta t - B(\vec{x}) t^2} \tag{3.12}$$

where,

$$B(\vec{x}) = f\alpha H \int d\vec{y}\gamma^2(\vec{x},\vec{y})D(\vec{y},0). \tag{3.13}$$

This approximation describes the $A(\vec{x},t)$ pulse as a function of the initial value of D.

Using this approximate solution for $A(\vec{x},t)$, we estimate the increase in memory cell population values after the infection is cleared. We take the value of $M(\vec{y},t)$ to be constant after time t_e when A has been reduced to half its initial value, in the tail of the pulse, and we round it to integer value.

$$M(\vec{y},t_e) = D(\vec{y},0)e^{(1-2f)\alpha\gamma Ht_e} - N(\vec{y},0)e^{-\gamma\alpha Ht_e} \tag{3.14}$$

This analytical result gives close agreement with memory cell growth levels given by our original model.

We estimate loss by integrating our analytical solution for the antigen population peak from $-\infty$ to ∞ (rather than starting at $t = 0$) to obtain:

$$L(\vec{x}) \approx A(\vec{x},0)\sqrt{\frac{\pi}{B(\vec{x})}}\exp\left[\frac{\beta^2}{4B(\vec{x})}\right]. \tag{3.15}$$

Note that extending the range of integration to $-\infty$ makes a relatively small difference in the result and simplifies this expression. Furthermore, it may in a certain sense be more accurate, as it accounts for the proliferation of antigen before it enters the lymph nodes.

3.2.1 Relaxation

On intermediate time scales the system relaxes, homeostasis adjusts naive cell number, and the naive cell population is turned over. These processes are considered fast enough to reach a steady state during the time between infections, but not so fast as to be a factor during an immune response. In the absence of antigen, the populations of effector and activated dendritic cells (which are both responsible for removing antigen from the body) relax back to zero ($E(\vec{y}) = 0$, $F^* = 0$ and $F = H$), as illustrated in Fig. 3.1. Though during an immune response N and M cells play an identical role (represented as D in Fig.3.1), during the homeostatic period, their differences become important. The memory cells are long lived and in the absence of antigen their population is static. Naive cells have a shorter lifetime than memory cells and die by apoptosis. As the naive cells die, homeostatic mechanisms stimulate the cells of the bone marrow to randomly repopulate the system with new naive cells. The repopulation is constrained by the total number of D cells, R:

$$R = \int \left[M(\vec{y}) + N(\vec{y})\right] d\vec{y} = M_{tot} + N_{tot} \tag{3.16}$$

This constraint is violated during an immune response as the lymphocytes rapidly proliferate, corresponding to the swelling of the lymph nodes. Once the antigen is cleared the total relaxes back to R. Thus, as memory cell populations rise,

homeostasis effectively depletes the naive cell population. The replacement of naive cell populations with memory cells with increasing age is described by Linton and Dorshkind [33].

3.3 Long Term Development

Next, using Eqs. (3.14,3.15,3.16) and simulated naive cell recycling, we study the long term adaptation of lymphocyte populations over the lifetime of the individual. Using these approximations, our model reduces to a cellular automaton describing the population changes of lymphocytes on the shape space after each infection under our homeostatic constraint, Eq. (3.16). Initially the system is composed of R naive cells. The naive cells randomly populate the shape space with uniform probability. The system is then inoculated with antigen at position $\vec{x}$ with probability $P(\vec{x})$. The corresponding loss is computed Eq. (3.15), as well as the change in the memory cell population Eq. (3.14). The naive cells are then redistributed with their number adjusted to satisfy Eq. (3.16). A subsequent inoculation of the same antigen will make use of these memory cells for a more rapid response, but an inoculation at another point in shape space will have a reduced number of naive cells with which to respond and the loss will be higher.

We monitor the evolution of loss on long time scales by considering a 70×70

lattice with $n = 36$ possible infections, at sites evenly distributed, indexed i, occurring with probability p_i. The infections are far enough apart that cross-reactivity is not a factor. The probabilities of infection are taken to have a few chronic infections that are very likely to recur, and many small rare infections. The probabilities are given by an exponential distribution:

$$p_i = \zeta e^{-i/\xi}, \tag{3.17}$$

where we set $\xi = 20/3$ and $\zeta = \sum_{j=1}^{n} e^{-j/\xi}$ normalizes the distribution over the discrete set of n infections. We choose a distribution of this form to have a mix of frequent and rare infections. We have used other distributions as well (e.g. a power law distribution), and obtain similar results. Different distributions alter the memory cell population growth rate, which effects the time scale for the onset of immunosenescence. Realistically the distribution of diseases and their respective infection probabilities is itself a dynamic coevolving system with new diseases constantly arising. In such a dynamic disease distribution, when the naive cell population is depleted there will be fragility similar to the observations reported here. With the kind of static distribution we consider here, in order for fragility to develop the rare diseases must have low enough probability that one of them is likely to be experienced for the first time once the naive cell population is depleted. Changing the numerical values of parameters in the model will in

general change the rate at which the naive cell population is depleted. We run the simulation for 400 infections drawn at random from the above distribution. Figure 3.2a (top) shows the loss $L(\vec{x})$ for each event in a representative sequence.

3.4 Immunosenescence

Figure 3.2b (top) illustrates the corresponding lymphocyte populations ($D(\vec{y}) = M(\vec{y}) + N(\vec{y})$) on the shape space at three stages in the adaptive development: initial, after 250 infections, and after 400 infections. The corresponding loss fields are illustrated below (these illustrate the loss which would be incurred for a subsequent infection as a function of the antigen characteristics $\vec{x}$). In the left figure D is strictly composed of naive cells. In the middle figure, D includes a mix of memory cells which form in the neighborhood of the inoculations, and the recycled naive cells. The right most figure is almost entirely depleted of naive cells. The bottom images show $L(\vec{x})$ for the naive state and after inoculations. These figures illustrate what the loss would be, given the D values in the figure above, for an inoculation at each point on the lattice (though we only consider the 36 points to be possible infections). Initially there are few vulnerabilities, associated with potentially large losses (red), in the system. Instead the system is uniformly protected. However, after 250 infections, the system develops structure and has

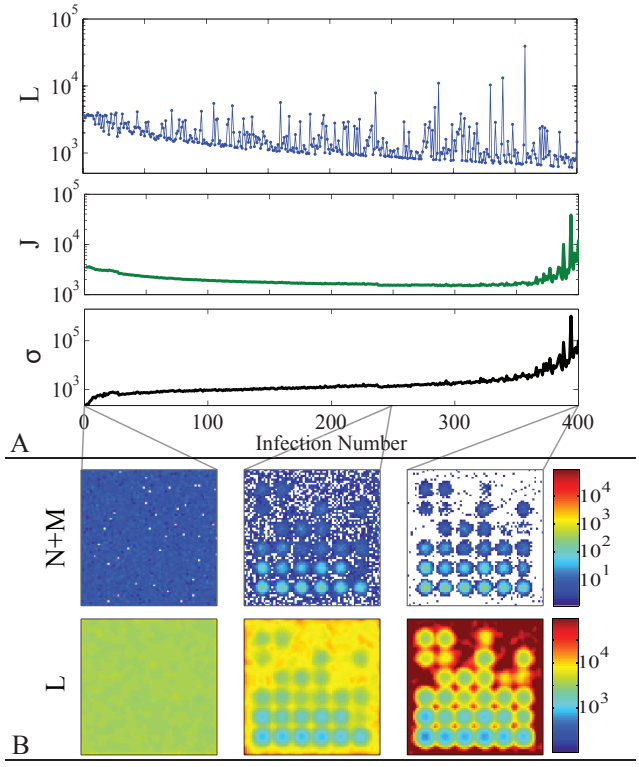

Figure 3.2: One realization of system development for 400 infections on a 70×70 lattice. There are 36 possible infections evenly distributed throughout shape space with $R = 33000$. The distribution of probabilities for the infections approximates an exponential, Eq. (3.17). In (a) the top curve illustrates the actual losses based on the history of infections. For most of the simulation, expected loss J, Eq. (3.18), tends to decrease, yet rare events are increasing in size resulting in increased variance σ Eq. (3.19). Eventually this results in catastrophic failure. Figure (b) illustrates the shape space representation of populated receptor sites in the immune system initially, after 250 infections, and after 400 infections (top), and the corresponding distributions of losses for subsequent infections (bottom). The initial configuration (left) is randomly populated by naive cells. After each infection there are elevated populations of memory cells in the vicinities of the infection site. The bottom figures illustrate how the immune system becomes skewed in favor of rapid response to repeated exposures at the expense of novel infections, by illustrating the immunological losses, Eq. (3.15), that would be incurred by inoculations at each lattice point before and after building up memory cell populations.

areas of high potential loss around the rare antigens. The points around the most common infections are well protected after 250 infections, indicating low values of loss (dark blue) in subsequent infections. However, because of the overall constraint on the number of cells, many outlying areas are left more vulnerable than they were initially.

Based on the probability distribution of infections, we calculate the expected loss J at each stage of the system's adaptation. Here J corresponds to the average value of $L(\vec{x})$ computed over the full spectrum of possible infections, and weighted according to the probability of each infection:

$$J = \int P(\vec{x})L(\vec{x})d\vec{x}. \tag{3.18}$$

The standard deviation σ gives a measure of the corresponding variation in the possible loss values:

$$\sigma = \sqrt{\int P(\vec{x})L(\vec{x})^2 d\vec{x} - J^2} \tag{3.19}$$

The expected loss J Fig. 3.2a (middle) initially decreases from the starting value, associated with random population of shape space. As the system adapts, J takes its minimum value at roughly 250 infections, which we refer to as the "optimal" state. In later stages J begins to rise, due to overspecialization. It is this increase which we associated with immunosenescence. Throughout the simulation adaptation is accompanied by a steady increase in the variability σ (Fig. 3.2a (bottom)),

associated with increasing breadth in the distribution of losses as the system becomes increasingly specialized. At the latest stages of the simulation the increase in σ sharpens, which is indicative of extreme vulnerability to rare events.

Figure 3.3 illustrates the cumulative statistical distribution of loss sizes obtained by combining data from 600 simulations of the form illustrated in Fig. 3.2. The initial state is characterized by a narrow (note the logarithmic axes) and flat distribution, which reflects the uniform coverage of shape space by the random population of naive cells. The blue curve corresponds to the optimal state, where the expected loss J takes its minimum value. Compared to the initial state, here the distribution of losses is both broader, and more variable, indicative of adaptation which optimizes the inherent tradeoff between reducing loss sizes for frequent events, at the cost of larger losses for less frequent infections, which arises because of the overall resource constraint (Eq. (3.16)). The red curve shows the result at the end of our simulation, when the system has overspecialized, and exhibits immunosenescence. In this case, the distribution of losses is extremely heavy tailed, corresponding to the increase in J. Any distribution containing very rare events leads to heavy tailed loss statistics as the naive cell population becomes depleted. This heavy tailed distribution of loss shows immunosenescence in the increased fragility of an aged immune system to as yet unseen diseases.

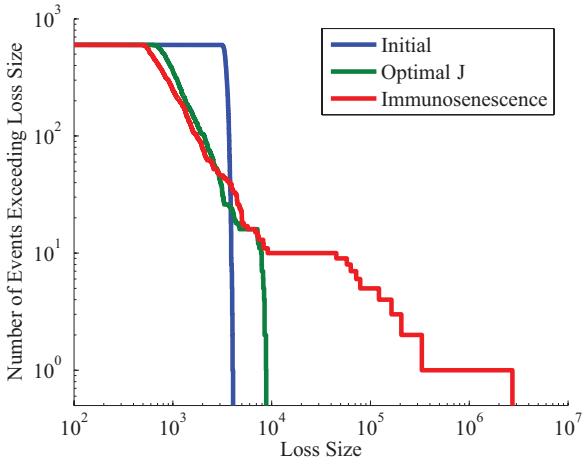

Figure 3.3: Distribution of losses over 600 realizations of the system. Results are shown after the first infection, after 250 infections (when J is at its lowest value, corresponding to the optimal state), and after 400 infections (corresponding to immunsenescence), in black, blue, and red respectively. The infection probabilities have the same distribution as in Fig. 3.2.

3.5 Connection to other Complex Systems

Our model is representative of the HOT mechanism [34, 35], in which robustness tradeoffs provide a mechanism for complexity and power laws through either deliberate design or biological evolution, both of which favor configurations which minimize loss, Eq. (3.18), subject to resource constraints, Eq. (3.16). The simplest examples are referred to as "Probability Loss Resource" (PLR) HOT models [36, 37, 38], which incorporate physically motivated relationships between resource allocations and loss sizes of individual events to define a constrained resource optimization problem involving a set of events with prescribed probabilities. In the cases which have been studied to date, resources have acted as barriers to propagation of cascading events, such as wildfires [39] or power outages [40]. In our case, the analogy is more akin to a sprinkler system, populated by lymphocytes, in the shape space of possible pathogens. Over time, adaptation leads to specialized states, through replacement of naive cells with memory cells, which are tuned to the history of past exposures. This results in a system which is increasingly robust to common disturbances, yet increasingly fragile to rare events–a key signature of HOT. In our model, this age correlated effect is a result of over specialization rather than an accumulation of defects. Other possible factors, such as deterioration, may contribute to immunosenescence as well, though it has been

experimentally observed that some symptoms are due to system dynamics [41].

Consequences of overspecialization were studied previously in a HOT model of evolution, based on Darwinian mechanisms [42, 43], leading to extreme vulnerability, similar to our observations here. In that case, offspring of lattice organisms evolved through random mutation relative to their parent lattice, and fitness was based on disturbances over the lifetime of individual lattices. Competition resulted in development of generalists and specialists. While specialists flourished during common circumstances, they experienced episodic extinction during rare events, which parallels the extreme fragility in our model associated with immunosenescence. In that case, the mutation rate itself was subject to mutation, and high mutation rates played an important role in rapid diversification and evolution following an extinction of the specialists. In the immune system, rapid mutation is associated with somatic hypermutation, which gives the daughter cells of lymphocyte stimulation a receptor that is a mutation of the parent's corresponding receptor. This gives rise to higher affinity, more efficient responses [44] and will be considered in future work.

While we have focused on immunosenescence, there are numerous additional robustness tradeoffs associated with the immune system. For example, the immune system has the ability to attack and remove non-self elements from the body with no prior knowledge of non-self features. Normally this is done with

little harm to the body itself. However, the immune system can make mistakes in recognition, leading to autoimmune disease, a fragility which would not be present if an organism had no immune system to begin with. In addition, on adaptive time scales, the ability to retain memory of past exposures enables development of effective vaccines, and reduces the severity of outbreaks of communicable diseases within populations. However, in some instances vaccinations may also lead to increased susceptibility to similar diseases [45, 44]. This "Robust Yet Fragile" behavior is a key feature of HOT, a statistical theory for complexity in designed, evolved, or adaptive systems. The immune system can be viewed as a complex system in which robustness tradeoffs play a central role in evolution of the basic operating mechanisms as well as adaptation of cell populations within an individual. We emphasize the importance of tradeoffs associated with a spectrum of possible events. Evolution and adaptation favor increased robustness to common disturbances, but this is inevitably paired with increased fragility, both to rare events as well as new opportunities for diseases and disturbances to hijack the system which would not be available were the system not in place.

Chapter 4

Pathogen Induced Tolerance

The response of the adaptive immune system of vertebrates [46] is a function of past infectious disease exposures. An immune response can have several different effects on future exposures: immunity for identical or nearly identical diseases, some amount of cross-reactive protection for similar diseases, no effect for unrelated diseases, and in exceptional cases an increased vulnerability. Cross-reactive protection is conferred when a secondary infection has chemicals with characteristics similar to those of the primary infection.

The adaptive immune system derives the ability to respond to new infections through a diverse population of cells, each having a distinct set of chemicals to which it can respond [28, 30, 29]. The mechanisms that generate this diversity also generate cells that will respond inappropriately to inert environmental chem-

icals (allergens), or even the body's own chemicals, thereby causing autoimmune disease. The mechanisms that generate the cellular diversity of the adaptive immune system need to be balanced with mechanisms of tolerance that prevent these inappropriate immune responses.

The dengue viruses are a disease system with the unusual property of increased vulnerabilities after the first exposure to dengue. Exposure to one of the dengue viruses primes the immune system to be vulnerable to a more severe form of the disease upon future exposure to the other dengue viruses. To explain this unusual dynamic we present and study a novel mechanism, "Pathogen Induced Tolerance," (PIT). In this mechanism the antigens from a primary infection also participate in the immune system tolerance mechanisms. The antigens of the primary infection bear chemical resemblance to the chemicals of the other dengue viruses and thereby tolerize the system to those viruses. Tolerizing the system in this way reduces the ability of the system to respond to the other viruses leading to a more severe disease states of either dengue hemorrhagic fever (DHF) or dengue shock syndrome. The PIT mechanism is shown to reproduce in a straightforward manner the key signatures of the dengue system.

In this chapter we use the dynamical model of the adaptive immune response developed in Chapter 3 and [24] to study the effects of cross-reactivity in a pair of infections (termed primary and secondary). The PIT dynamic is robust with

respect to the choice of immune response model. The use of a dynamic model provides a tool not only for illustration of the dynamics, but also makes explicit the reactions we are considering, can lead to quantitative predictions, and suggest experiments. This model uses differential equations to model the behavior of antigen proliferation, lymphocyte stimulation, antigen removal by effector lymphocytes, and effector death. Our model includes the dynamics of the diverse population of lymphocytes which we organize using generalized shape space models [31]. We introduced and studied the model previously in the context of immunosenescence, focusing on long term robustness and fragility tradeoffs associated with the natural adaptive mechanism assuming negligible interactions between infections [24]. This study focusses on fragilities induced by cross-reactivity on short-time scales.

4.1 Negative Selection

The adaptive immune system is composed of B and T white blood cells (i.e. lymphocytes). These cell types derive their self, non-self discrimination ability from the binding specificity of their receptors: T cell receptors for T cells, and membrane bound antibody for B cells. These receptors are assembled randomly from gene segments (VDJ recombination), producing a population of pre-naive cells, in which each individual combination has a different binding specificity.

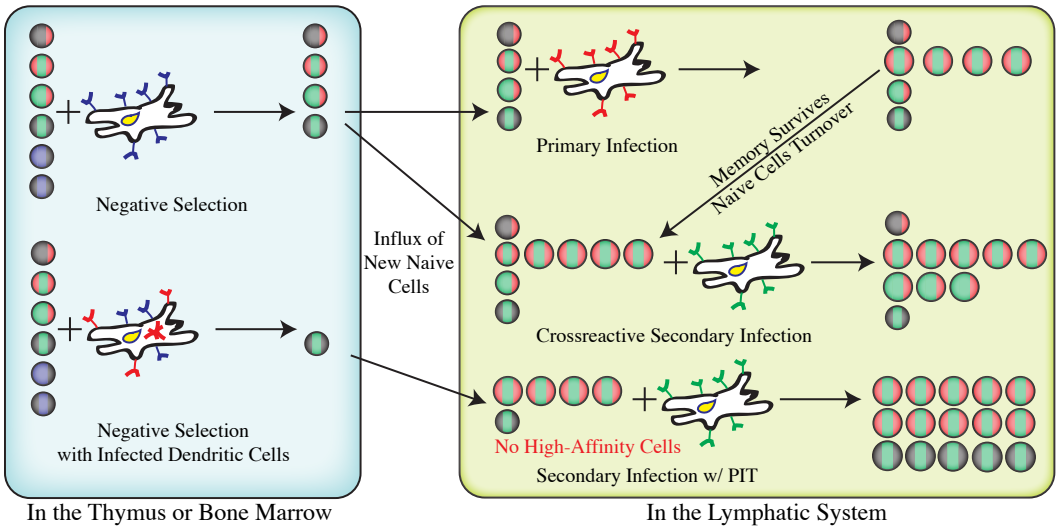

Figure 4.1: Negative and positive selection under primary, heterologous secondary, and heterologous secondary with PIT phenotype infections. Colored circles represent lymphocytes. The colors in the circles represent what colors of antigen will stimulate the lymphocytes, the greater fraction of matching color the higher affinity for that color antigen. In the left box representing the thymus or bone marrow the diverse population of pre-naive cells is shown containing some autoreactive cells that will bind to self-antigen shown in blue. The mature naive cells in the right do not contain any cells that recognize blue antigen. The system then experiences an infection with a disease whose antigens are represented as red. The lymphocytes with high affinity for red antigen multiply most rapidly, remove the antigen from the body and leave behind a population of memory cells (large spheres). The influx of naive cells from the thymus and bone marrow causes a turnover and replenishment of the naive population. For a secondary heterologous infection with an disease whose antigen is represented in green, having some crossreactivity with the red antigen the response should involve the high affinity cells for green and some of the memory cells that have a low affinity for green. This secondary response should be less severe than the primary infection. The bottom diagram in the left box shows the case if the antigen from the primary infection is also presented in negative selection. In that case only cells that have no affinity, high or low, for self antigen or antigen from the first infection, enter the naive pool. No high affinity naive cells will be entering the lymphatic system creating the PIT phenotype where only low affinity cells will be available to fight the heterologous secondary infection.

This population having randomly arranged receptors contains a large fraction of cells which bind to the body's own chemicals.

These autoreactive pre-naive cells are triggered to die by apoptosis when they recognize antigen (Negative Selection). This maturation and selection process takes place in the Thymus for T cells and in the bone marrow for B cells. Fig. 4.1 illustrates the negative selection process in the left hand box. As many as 90% of the pre-naive cells are removed in this manner [47]. Negative selection is facilitated by dendritic cells which present the native antigens to the pre-naive cells. The pre-naive cells that are not triggered to die, mature to become short-lived naive cells. This diverse population, having receptors composed of random combinations of genes, gives the immune system the ability to respond to many pathogens. The roll of negative selection in the immune system is shown pictorially in the top right image of Fig. 4.1.

4.2 Crossreactivity

In addition to immunity for a homologous secondary infection, the memory cells can have a positive effect on heterologous secondary infections depending on how strongly they bind to the new antigen. There are numerous examples of diseases that have such a cross-reactivity for each other [48] including cowpox and

smallpox, influenza A and hepatitis C, rotavirus and HIV-1, and choriomeningitis virus and pichinde virus. This crossreactive effect typically results in a shorter disease with fewer symptoms. This crossreactive infection is shown pictorially in Fig. 4.1 in the middle of the right hand box. Here the memory cells from the previous infection are low affinity and provide some additional protection.

4.3 Pathogen Induced Tolerance

In some disease systems a negative effect on heterologous immune responses has been observed [49, 50]. Dengue is an example of such a disease system. There are four dengue virus serotypes. A primary exposure to one typically results in dengue fever and a long lived immunity to that serotype. For a period of a few months [51, 49] there is also an observed beneficial immunity to heterologous infections with the other dengue serotypes. This cross-reactive protection is short lived and eventually the system is left in a fragile state, vulnerable to dengue hemorrhagic fever (DHF) [49, 52]. DHF is primarily a disease afflicting children. The dengue virus also is able to penetrate and infect dendritic cells, raising the possibility that dengue epitopes could be presented to pre-naive cells.

Typically between infections the populations of naive cells are replaced by the constant influx of new naive cells. This turnover of naive cells can take several

months, the time scale being set by the influx of new cells. The naive influx is highest in children and decays with age.

The central hypothesis of this chapter is that dendritic cells infected with dengue virus may be presenting pathogenic antigen during negative selection. This is pictorially represented in Fig. 4.1 in the left box at the bottom. The naive cells that would be high affinity for the secondary infections are now absent from the naive influx due to their crossreactivity with the antigens from the primary infection. As the naive population turns over the naive cells that would have provided a high affinity response to the secondary heterologous infection decay in number leaving the system vulnerable to a more severe form of disease. This "Pathogen Induced Tolerance" (PIT) is a vulnerability that may also be present in other disease systems.

4.4 Cross-Reactive Dynamics

We use the mathematical model of the immune response developed in Chapter 3 and [24]. In that chapter we considered a sequence of 400 unrelated infections [24] with no cross-reactivity. In this study we look at the effects of a sequence of two infections that have a chemical similarity.

In this study we look at the effects of a sequence of two infections that have

a chemical similarity. We ignore the long term repertoire thinning discussed in Chapter 3 as it is relevant for memory accumulation over a lifetime of infections. Here we are interested in a sequence of only two infections that have some degree of cross-reactivity. We also assume that the primary immune response completely ends before any secondary infection begins.

The reactions considered in this chapter are shown diagrammatically in Fig. 4.2. From the left: pre-naive cells P can be stimulated by antigen presented on dendritic cells (H) to apoptose. This negative selection reaction acts to remove autoreactive cells. If a pre-naive cell survives negative selection it will mature to a naive cell (N). Naive cells can be stimulated in the same way by H but proliferate into memory (M) and effector cells (E). Naive cells that do not bind antigen must compete for limited survival factors with the constant influx on new naive cells coming from the bone marrow and thymus and will eventually die by apoptosis. The naive population is turned over in this manner every few months [47]. Memory populations are long-lived but otherwise identical in our model to naive cells. The memory cells can be stimulated in the same manner as naive cells, proliferating into more memory cells and effector cells. The effector cells are short-lived and do the work of removing the antigen (A) from the body. Antigen growth via reproduction of the associated pathogen is also shown on the far right of Fig. 4.2.

The model equations describing these populations and the illustrated reactions are presented in Eqs. 3.2-3.6. Parameter estimations for this chapter are listed in Appendix A.

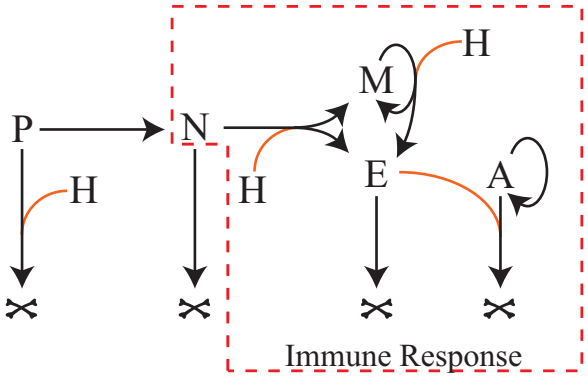

Figure 4.2: This flowchart summarizes the reactions considered in our model. The leftmost reaction shows pre-naive cells (P) subjected to negative selection. Those pre-naive cells that survive negative selection become short-lived, continuously recycled naive cells (N). The red box surrounds reactions taking place during an immune response and modeled with differential equations. The reactions shown in orange are affinity dependent.

As the reactions considered here are common to both T-cells and B-Cells, we do not make a distinction between them in our model. This technique has been used in past generalizations [29]. Additionally, we do not consider many immune system effects such as T-help, somatic hypermutation [44], or the complexities of germinal center reactions [53, 54]. Including T-help would if anything make the consequences of the PIT phenotype more severe as helper T-cells could also suffer the PIT phenotype. The variations in the dynamics of germinal center reactions

are considered to be primarily a function of the affinity of cells for antigens and thus the effects of the germinal center reactions are implicitly assumed in the model. Somatic hypermutation could lessen its effects on PIT for B cells by evolving low affinity B cells to become high affinity, but the reaction will still be worse for PIT phenotype than for a primary infection. T cell responses do not utilize somatic hypermutation.

In order to model an immune response with a large diversity of lymphocytes we again use the generalized shape space technique of Oster and Perelson [31]. We again use only two dimensions for illustrative purposes and consider a very small region of the total shape space in the neighborhood of the antigen vector for the primary infection. Here we also are not concerned with the stochastic effects associated with rare naive cells in immunosenescence and use a flat continuous distribution of naive cells. The degree of cross-reactivity of two infections is described in this chapter in units of b the term that sets the shape space scale in Eq. 3.1. The simulations in this chapter were performed on a 96×96 lattice.

4.4.1 Primary Infection

The basic behavior of the model for a single infection is shown with the dashed black curve in Fig. 4.3 and the memory accumulation shown in Fig. 4.4. Fig. 4.3 shows the antigen response curve $A(\vec{x}, t)$ for the primary infection where the initial

conditions are a uniform field of naive cells and no memory cells, Fig. 4.4 (left). Initially there are no effector cells the antigen growth is approximately exponential. This curve turns over however as the effector cell population increases.

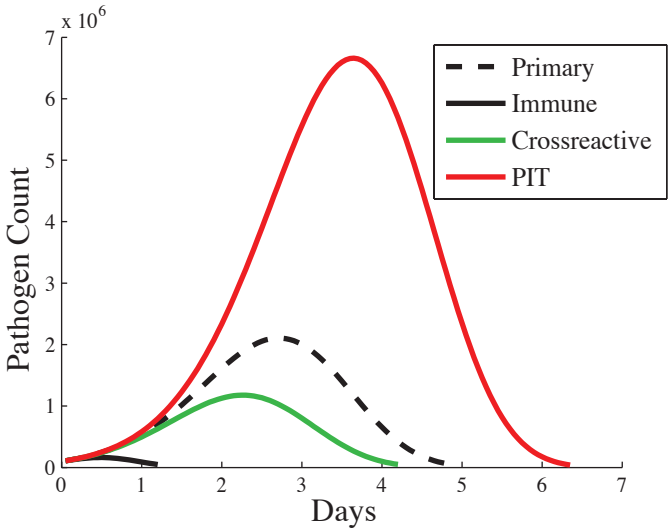

Figure 4.3: Antigen response curves $A(\vec{x}, t)$ for four scenarios of the model. The dashed black curve shows the response curve for the initial exposure (Primary), while the solid black curve shows the response to a second exposure of the same antigen (Immune). The green curve shows the response to a related disease (Cross-reactive) following the initial exposure. The shape space position in relation to the primary antigen is shown with the green marker in the shape space drawn in 4.4 and 4.7. The red curve corresponds to the same cross-reactive infection as the green curve but with the PIT phenotype, where the antigens from the primary infection have acted in negative selection. The red curve is a more severe disease state, with greater magnitude and longer infection.

When the immune response has cleared the antigen from the system, long-lived memory cells are left behind. Figure 4.4 shows the distribution of naive and memory cells around the pathogen in shape-space, before and after the immune

response. Before the infection the distribution of lymphocytes is a uniform low level (all blue) field consisting only of naive cells. After the immune response there is an accumulation of memory cells that will survive indefinitely. This peak is centered on the antigen vector of the primary infection, as naive and memory cells with receptor vectors close to that proliferate most rapidly.

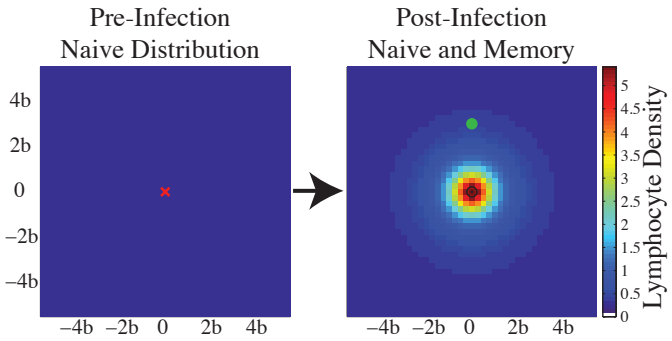

Figure 4.4: The density of naive and memory lymphocytes in the shape space before and after an infection. The vector $\vec{x}$ for the primary infection is shown as a red x in the center of the left figure. Initially the distribution is uniform consisting of only naive cells. After the immune response the memory cell population survives indefinitely. The memory cells are peaked around the antigen vector as the closest naive and memory cells have the highest proliferation rate. The green circle marks the locations of secondary infection in Fig. 4.4. Only a small portion of the total shape space, in the neighborhood of the primary infection, is shown. The shape space distance is measured in units of b the length scale for the function of affinity given shape space distance.

4.4.2 Immunity

When the system is re-inoculated with the exact same antigen (center of Fig. 4.4), the memory cells provide an enhanced response. In Fig. 4.3 the solid

black line shows the response to a homologous secondary infection, where the initial memory and naive cell populations are shown in the right hand image in Fig. 4.4. The antigen pulse in Fig. 4.3 is shorter and lower in magnitude, a less severe disease for a shorter period of time. This is due to the much faster effector cell response.

It should be noted that our model approximates the short term dynamics of memory cells and naive cells as being identical. The more rapid response in Fig. 4.3 is due to the larger initial number of high affinity memory cells rather than an intrinsic difference in stimulation rate for memory cells versus naive cells.

To quantify the severity of an infection we use the loss measure defined in [24]. This quantity is the integral over the $A(\vec{x}, t)$ pulse:

$$Loss = \int_0^\infty A(\vec{x}, t)dt. \tag{4.1}$$

The Loss is proportional to the resources the pathogen consumes, and the total amount of toxin the pathogen secretes over the course of the infection. For the primary and secondary infections in Fig. 4.3, the loss was 4.9×10^6 and 1.5×10^5 respectively with units of antigen $\times$ days. The presence of memory cells at the start of the second infection reduced the severity of that infection.

4.4.3 Cross-Reactivity

The memory cells left after the primary infection can have some affinity for heterologous secondary infections. This phenomenon is known as cross-reactivity or polyspecificity [55]. Cross-reactivity of memory cells is typically beneficial, such as the historic practice of vaccinating against smallpox with inoculation of the virus that causes cowpox. (Memory cells can have a negative cross-reactive effect if the antigen from the primary infection bears similarity to the self-antigens of the body, thereby inducing autoimmune disease [56]. We do not consider autoimmune effects here.)

To study the effects of cross-reactivity in the shape space picture, the vectors for the antigens of the primary and secondary infections must be similar. Mathematically the distance between the two shape space vectors must be within several b, the term that sets the shape space scale. We look at a range of degrees of similarity for heterologous secondary infections.

The green circle drawn on the memory and naive distribution of Fig. 4.4 corresponds to the location of the cross-reactive curve in Fig. 4.3. This antigen response curve is less severe than the primary infection due to the presence of the low affinity memory cells left from the primary infection.

As the shape space position of the secondary antigen moves away from the

primary antigen, the infection becomes more severe. The antigen pulses are progressively longer in time and with larger maxima until the secondary antigen is far enough away that the curve is equal to the curve for the primary infection.

The blue dashed curve in Fig. 4.5 shows the loss as a function of antigen position for a range of similarities for heterologous secondary infections. This curve asymptotically and monotonically approaches the loss of the initial infection as the secondary antigen moves away from the primary antigen in shape space. In the limit of zero antigenic difference we see the result discussed in Section 4.4.2 for a homologous secondary infection. Cross-reactivity provides some immunity to diseases closely related to ones we have previously encountered.

4.4.4 PIT Dynamics

Here we show the expected effects of dendritic cells presenting pathogenic antigen to pre-naive cells: pathogen induced tolerance (PIT). This provides a mechanism by which a primary infection can leave the repertoire in a state vulnerable to heterologous infection.

To describe PIT we include negative selection in our model. We model negative selection in the shape space as a perfect process removing all immature lymphocytes within a radius r_n of the presented antigen. Figure 4.6 shows this effect on the distribution of naive cells. The pre-naive cells are derived from stem

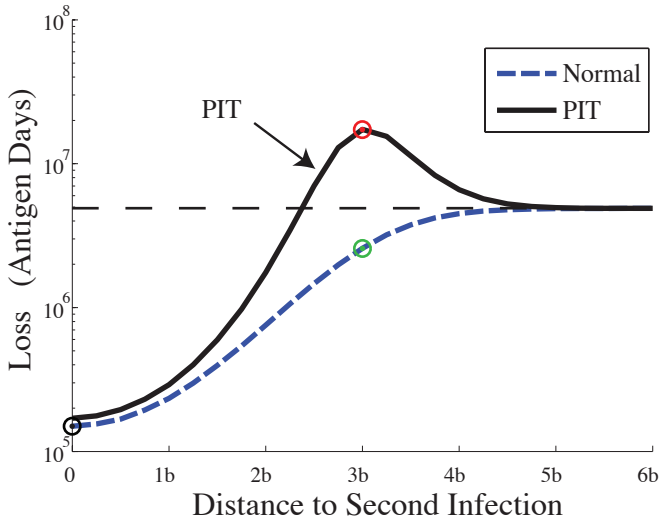

Figure 4.5: The loss for secondary infections as a function of shape space distance from the primary infection to the secondary infection. The blue dashed curve illustrates the losses on the naive and memory distribution in the right hand image of Fig. 4.4. The blue curve shows the loss monotonically converging to the value for the primary infection (grey dashed line) as the distance increases. The solid black curve shows losses for the negatively selected PIT phenotype naive and memory cell distribution shown in the right hand image of Fig. 4.7. The PIT vulnerability is seen on the black curve when the loss for a secondary infection exceeds the loss for a primary infection. The circles on these plots correspond to the markers for shape space positions for the secondary epitopes in Fig. 4.4 and Fig. 4.7 .

cells in the bone marrow, uniformly populating the shape space with their random receptors shown pictorially on the left. An antigen presented during negative selection is shown as a red x at the center of this distribution. The right hand image shows the naive cells that have matured. This distribution has a hole with radius r_n around the presented antigen where pre-naive cells were prevented from maturing.

Treating negative selection as a perfect process gives a hard edge in the lymphocyte density profile. This is in contrast to the smooth memory profile shown at right in Fig. 4.5. This contrast is due to multiple factors. Pre-naive cells are continuously in the thymus or bone marrow being repeatedly presented antigen while naive cells spend a large fraction of their time in the periphery. The continual presentation makes negative selection a more efficient selection process. Second, the smoothness of the memory profile is due to multiple divisions of lymphocytes with low affinity cells dividing less rapidly when presented antigen. For PIT phenotype to occur the approximation of a perfect process need not be completely accurate, autoimmune disease though rare, does occur. All that is required is significant depletion.

In order for negative selection to provide a protection against autoimmune disease the radius of cells that are positively selected r_p, must be smaller than r_n:

$$r_p < r_n. \tag{4.2}$$

If this were not the case, cells on the edge of the hole generated by negative selection, Fig. 4.6 would be positively selected by self-antigens once mature. This would generate an immune response against those antigens, thereby generating autoimmune disease. Insuring that $r_p < r_n$ prevents the maturation of autoreactive lymphocytes and autoimmune disease.

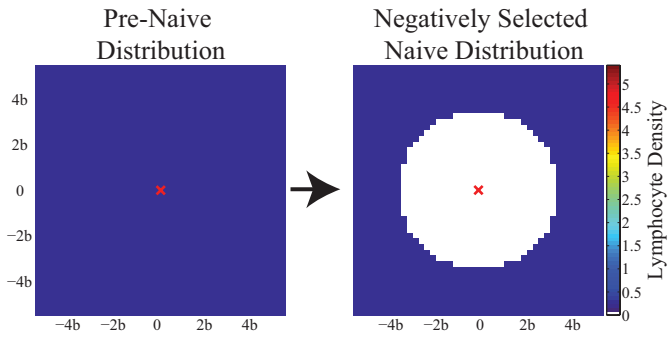

Figure 4.6: Before and after negative selection: The left hand image shows the source of pre-naive cells. This is a uniform distribution. The shape space vector of antigen presented during negative selection is shown with the red x. The population of naive cells that emerge after surviving negative selection is shown at right. We have modeled this process as being perfect, eliminating all cells within radius r_n that are likely to be positively selected by that antigen were it encountered in the body.

The signature of an infectious disease whose antigens are presented to not only naive and memory cells, but to pre-naive cells as well is shown in Fig. 4.7. This figure shows the naive and memory cell population development for an infection that is incorporated into negative selection. This may happen from an infectious disease whose antigens persists for long periods in the body, such a virus with a long latent phase, a chronic bacterial infection, a pathogen that infects dendritic cells, or frequent re-exposure to the initial infectious agent.

The antigens from such an infection would not only be presented in the lymph nodes to stimulate a response, but also to the pre-naive cells. The two left images in Fig. 4.7 repeat the reactions in Fig. 4.4 as the primary infection would not

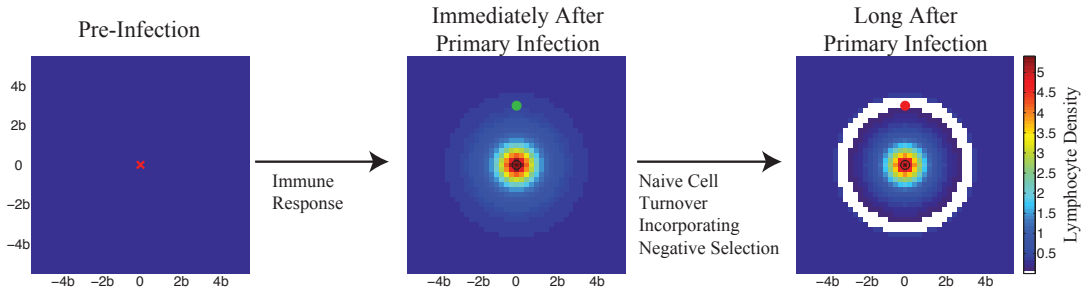

Figure 4.7: The development of vulnerability after an infection whose antigen is incorporated into negative selection. The initial response to the primary infection is shown in the first two images. When the antigen participates in negative selection over the time scale of naive turnover, the lymphocyte density shown in the middle image will progress to the image at right. As the naive population is turned over, the replacement naive cells have a hole around the antigen from the first infection. The radius of the hole r_n must be larger than the radius of positively selected cells in order for negative selection to aid in prevention of autoimmune disease.

differ. The middle distribution in this case however is short-lived. As the naive cell population is turned over the replacement naive repertoire has a hole centered on the antigen from the infection.

The right image in Fig. 4.7 shows the memory cells accumulated during the immune response in the center, with a naive cell distribution having a hole centered on the antigen from the primary infection giving the ring surrounding the memory cells.

A heterologous infection with antigen in the region where there are no memory cells and no naive cells in the right hand image of Fig. 4.7 will cause severe disease as the system is now unable to produce any high affinity effector cells. The

immune system has become more tolerant to a subset of secondary infections due to the primary infection. This will lead to more severe disease from that subset of infections. The antigen response curve for an infection of this type is shown in red in Fig. 4.3. This curve has a far greater amplitude and lasts for a much longer period.

The loss as a function of the shape space distance between the primary and secondary infections for the PIT phenotype is plotted in black in Fig. 4.5. As can be seen in the figure, for parameters used in this study, the loss exceeds the primary loss by as much as four times for serotypes with shape space distance greater than $2.25b$.

This behavior is summarized in Table 4.1. Note from Table 4.1 that this dynamic is symmetric. Primary inoculation with A or B induces tolerance and hence vulnerability to B or A respectively.

Immediately following the primary infection the curve describing loss as a function of antigen similarity is given by the blue curve in Fig. 4.5. In the case of PIT this blue curve is short-lived and develops into the black curve as the naive cell population is turned over and the repertoire progresses from the middle image of Fig. 4.7 to the right hand figure.

Time Scale of PIT Development

The time scale of this PIT formation is set by the rate of influx of new cells (I). The rate of exponential decay (d) for populations not being added to (naive cells with affinity for the primary antigen) is given by:

$$d = \frac{I}{\kappa}, \tag{4.3}$$

where κ is the equilibrium number of cells in the system [14]. Normally the influx replaces the cells lost to attrition. However, with the antigen from the infection being presented in negative selection there will be no replacement. The time scale for PIT generation is therefore set by $1/d$.

Thymic influx has been show to decay exponentially with age [57]. This gives us an age dependent PIT development time scale:

$$\frac{1}{d(a)} = \frac{\kappa e^{ca}}{I_m}. \tag{4.4}$$

where a age, I_m is the maximum influx of new naive cells, and the constant c is the rate of decay of output of new naive cells with age (about 3% a year for thymic output). This age dependent effect indicates children will tend to develop the PIT phenotype more rapidly. Naive turnover in a young person takes place over a period of several months. Thus the antigen from the primary infection must be presented in negative selection for at least this long in order for the hole

Primary Antigen	Primary Infection		Secondary Infection			
			Before Turnover		After Turnover	
	A_a	A_b	A_a	A_b	A_a	A_b
A_a	-		+	+	+	- -
A_b		-	+	+	- -	+

Table 4.1: Phenomena predicted by model. A_a and A_b separated by a distance of around $3b$ in shape space. Normal infection and response (-), Immunity (+), Severe infection (- -).

to form. In the elderly where $1/d(a)$ is much longer, if the antigen presentation is temporary, the PIT is much less likely to form.

Pathogen Induced Tolerance (PIT) is a mechanism that can lead to heterologous secondary infections being more severe than primary infections. The development of the PIT phenotype consists of an infection and normal immune response, followed by the presentation of antigen from that infection to pre-naive cells. Initially heterologous secondary infections show no vulnerability but as the naive pool is turned over with the influx of new cells, naive cells with affinity for the primary antigens are lost. This turnover time is set by the influx of new cells, is given by Eq. 4.4, and is expected to be on the order of a couple months for children. The influx of new naive cells declines rapidly with age. The loss of naive cells with affinity for the primary infection thus is most rapid in children. For heterologous secondary infections, if an infection has antigens that have an intermediate cross-reactivity with the primary infection, where the memory from

the primary infection is low affinity for the second infection and the naive cells that would be high affinity are absent, the secondary infection can be very severe.

This vulnerability is a consequence one of many tradeoffs in the adaptive immune system. Here the necessity of a diverse naive population requires tolerance mechanisms to prohibit inappropriate responses to self. These tolerance mechanisms can then also act inappropriately, creating vulnerabilities such as PIT. There is no vulnerability to the original pathogen with the PIT phenotype because even without the high affinity naive cells there are high affinity memory cells left that provide immunity, Fig. 4.7 (right).

The characteristic behavior of PIT is robust to our choice of immune response model and requires only that negative selection is more efficient than positive selection. This is represented mathematically by Eq. 4.2. Biologicaly we know this must be true for negative selection to help prevent autoimmune disease. If pathogenic antigen can stimulate these low affinity cells in positive selection, then the ubiquitous self antigens should also stimulate low affinity cells, leading to autoimmune disease. Additionally, the requirement in Eq. 4.2 also selects the highest affinity naive cells in an immune response. Quantitative predictions will become more accurate as measurements are made on the degree of cross-reactivity for different disease epitopes, and there is better characterization of the immune response and lymphocyte repertoire.

The lasting effects of pathogen induced tolerance (PIT) could vary widely. For an antigen that is unable to grow, such as a biologically inactive vaccine, or an antigen whose associated pathogen has been completely removed from the body, the PIT phase will be short-lived. The remaining antigen may degrade before the naive turnover is complete and the PIT vulnerability may never develop in this case. However, many viruses continue to live in the body, asymptomatically, at low levels indefinitely after the immune response [58, 59]. This is known as the asymptomatic or latent phase of the infection. If a virus is living in the body at low levels its antigens should be active in negative selection. Additionally, in areas where reinfection is common there could be a prolonged presentation of antigen even with immunity.

4.5 Dengue

While the PIT mechanism could be active in a number of disease systems the dengue system matches the signature of PIT. There are four closely related dengue virus serotypes. Infection with one serotype generates dengue fever and immunity to subsequent homologous infections. For a period of a few months [51, 49] there is also an observed beneficial immunity to heterologous infection with the other dengue serotypes. As predicted by our model this beneficial effect

is observed to be short-lived and the system is observed to subsequently evolve to a state where infection with another serotype can progress to a more severe Dengue Hemorrhagic Fever (DHF) [49, 52]. DHF like the PIT phenotype is also observed to affect children disproportionally [60].

Two additional factors increase the likelihood that dengue may be an example of Pathogen Induced Tolerance. One, dendritic cells are highly permissive to the dengue virus. Since dendritic cells present self-antigen during negative selection this enhances the likelihood of dengue antigens taking place in negative selection. The second factor is that dengue is a constant endemic threat in many of the areas it is found, increasing the likelihood of re-exposure to antigens that can maintain the PIT phenotype, even for short lived antigens.

While there are many proposed mechanisms for the dengue pathogenesis [61], the PIT mechanism is unique in that it matches all the signatures of the dengue system described here and provides simple explanations for much of the observed behavior. The absence of high affinity naive cells in the PIT phenotype could be responsible for the difference between dengue fever and dengue hemorrhagic fever.

Chapter 5

Conclusions

Study in theoretical immunology can be viewed broadly in three categories:

- Quantitative modeling
- Creating mathematical tools immunologists need to measure the parameters for quantitative models
- Explaining the system architecture[1] of the immune system.

Quantitative models can be used in medicine to reduce the amount of guess and check needed in development. Departure from the predictions of quantitative models can help biologists and immunologists make new discoveries. Quantitative models can also be used to suggest new experiments that can be done to

[1] the word design in biology now has a different meaning

discriminate between two different theoretical models that yield similar results.

To properly calibrate quantitative models, quantitative experiments are needed. This is uncommon in immunology. The most quantitative measurements in immunology are typically given as a percent change from a control, leaving the results open to interpretation. Making quantitative measurements in immunology can be more easily accomplished with the aid of models, fitting data to a model. The immunologist also needs statistical tools for fitting parameters.

The most ubiquitous tool in immunology is flow cytometry. It gives information on the simultaneous expression levels of different biological chemicals. It is presently used most often for counting the number of cells with florescence levels above or bellow thresholds. Applying structured population dynamics tools would allow connecting the molecular systems biology of these cells with the population dynamics of the system.

Theoretical modeling allows the scientist to ask questions of what the system would do if it operated differently, yielding insight into how and why it came to act the way it does. With so many tradeoffs and constraints this area of research in system architecture is quite complex. Scaling laws for example in the immune system have identified the smallest immune system possible given the specificity of antibody-antigen binding. This matches with the size of the adaptive immune system of a tadpole. Smaller than this and the system has a low probability of

being able to discriminate between self and non-self.

While UCSB's commitment to interdisciplinary studies has made this work possible, the lack of a medical school or immunology department has made it difficult to obtain the experimental results needed for calibrated models. In a research environment where the theoretician and the experimentalist interact there can be much more rapid progress made toward alleviating the pain and deaths associated with immune system disorders and the diseases the immune system fights.

At the moment only four of the world's immunology research centers have established theory groups. The cost of a theory group is likely miniscule in comparison to maintaing an animal lab. Society at large would benefit from every immunology research center having a theoretician. Unfortunately there are not yet many qualified researchers in the field and there is not a well defined pathway for training new PhDs. The NIH however has a funding initiative *Mentored Quantitative Research Development Award* (K25) to train researchers in the physical sciences to perform research in biology.

There is an abundance of work to be done in this field, so far we have only scratched at the surface, and the effects should improve the quality of lives of people ranging from the affluent Northern Europeans suffering from autoimmune diseases due to their lack of exposure to pathogens, to children in equatorial

regions suffering from dengue hemorrhagic fever.[2]

[2]One symptom of dengue hemorrhagic fever is "coffee ground vomit." Obviously we need to prevent that from happening.

Appendix A

Calibration Information for Chapter 4

Here we present equations for estimating seven of the model parameters given in Table A.1. These equations are derived from seven related quantities which can be approximated from the model equations. Those approximations are then

inverted to solve for the model parameters:

$$N(\vec{y},0) = \frac{N_t F}{l^d}; \tag{A.1}$$

$$r_n = \left[\frac{pN_t}{N(\vec{y},0)}\frac{\Gamma(d/2+1)}{\pi^{d/2}}\right]^{1/d}; \tag{A.2}$$

$$b = r_n \frac{1}{\sqrt{2ln\left(\frac{EDT}{MDT}\right)}}; \tag{A.3}$$

$$\beta = \frac{2}{t_e} ln\left(\frac{A_m}{A(\vec{x},0)}\right)\left[1+\sqrt{1+\frac{ln(2)}{ln\left(\frac{A_m}{A(\vec{x},0)}\right)}}\right]; \tag{A.4}$$

$$f = \frac{1}{2} - \frac{MDT}{ln(4)t_e} ln\left(\frac{\Delta mem[2\ ln(\frac{EDT}{MDT})]^{d/2}}{pN_t}\right); \tag{A.5}$$

$$\gamma_{max} = \frac{MDT\ \beta^2[2\ ln(\frac{EDT}{MDT})]^{d/2}}{4fln(2)pN_t\Gamma(d/2+1)ln\left(\frac{A_m}{A(\vec{x},0)}\right)}; \tag{A.6}$$

$$\alpha H = \frac{ln(2)}{MDT\ \gamma_{max}}. \tag{A.7}$$

The input parameters are:

- p, The specificity of the adaptive immune system is the probability that a randomly chosen lymphocyte and antigen bind strongly enough to stimulate the lymphocyte. We set p equal to 10^{-5} [62].

- N_t, the total number of naive lymphocytes. We set N_t equal to 2×10^7, which is the value for a mouse [63]. This value will be higher in a human making the PIT effect more severe.

- MDT, the doubling time for the highest affinity lymphocytes. We set MDT

equal to 6 hours, a standard estimate [46].

- EDT, the doubling time for the highest affinity self reactive lymphocytes, the lymphocytes on the edge of the sphere of negative selection. This must be at least as large as the naive cell lifetime. Incorporating T-help might relax this condition. We used EDT equal to 15 weeks.

- t_e, the length of time it takes to clear an infection. We used t_e equal to 10 days.

- A_m, the highest concentration of antigen during the primary infection. We set A_m equal to 10^7 [64].

- Δmem, the accumulated memory cells from a primary infection. We used Δmem equals 5000. The approximation for Δmem is order of magnitude.

The parameters MDT, EDT, t_e, A_m, and Δmem are approximated from the model using a Gaussian approximation for the $A(\vec{x}, t)$ pulse. The approximate equations (not shown here) for these parameters are then inverted to obtain the above equations. Additionally, the equations contain computational parameters d the dimension of the shape space, F the fraction of the total shape space we simulate, and l^d the number of lattice sites in the simulation. In the simulations of Chapter 4 $d = 2, F = 8.1 \times 10^{-5}$, and $l^d = 96 \times 96$. We expect the qualitative behavior of

Parameter	Value
$N(\vec{y}, 0)$	0.3 cells per lattice site
$A(\vec{x}, 0)$	10^5 cells
b	4 lattice sites
β	1.9 day^{-1}
αH	255 cells
γ_m	0.01 cell^{-1} day^{-1}
δ	0.01 day^{-1}
f	0.397
r_n	13.9 lattice sites

Table A.1: Values of parameters used in PIT model simulations. Note that the product αH is listed rather than listing the parameters individually. Only the product arises in this model. H is the number of sites occupied by antigen during an immune response and α is a factor accounting for the difference in rates for the two affinity dependent processes: stimulation and antigen removal. The qualitative behavior of the model is not especially sensitive to precise parameter values.

the model to not be sensitive to precise values.

Bibliography

[1] D. P. Strachan, BMJ **299**, 1259 (1989).

[2] J. F. Bach, N Engl J Med **347**, 911 (2002).

[3] T. M. Ball et al., The New England Journal of Medicine **343**, 538 (2000), PMID: 10954761.

[4] P. A. McKinney et al., Diabetic Medicine: A Journal of the British Diabetic Association **17**, 236 (2000), PMID: 10784230.

[5] H. J. Bodansky, A. Staines, C. Stephenson, D. Haigh, and R. Cartwright, BMJ (Clinical Research Ed.) **304**, 1020 (1992), PMID: 1586783.

[6] A. Staines et al., Archives of Disease in Childhood **76**, 121 (1997), PMID: 9068300.

[7] C. Braun-Fahrlnder et al., Clinical and Experimental Allergy: Journal of the British Society for Allergy and Clinical Immunology **29**, 28 (1999), PMID: 10051699.

[8] A. A. Like, D. L. Guberski, and L. Butler, Diabetes **40**, 259 (1991), PMID: 1899407.

[9] S. F. G. Zorzella, J. Seger, D. R. Martins, A. C. Pelizon, and A. Sartori, Memórias Do Instituto Oswaldo Cruz **102**, 931 (2007), PMID: 18209931.

[10] J. Kero, M. Gissler, E. Hemminki, and E. Isolauri, J Allergy Clin Immunol **108**, 781 (2001).

[11] C. R. Simpson et al., Clin Exp Allergy **32**, 37 (2002).

[12] D. V. Serreze et al., J Immunol **166**, 1352 (2001).

[13] J. F. Bach, Cell Immunol **233**, 158 (2005).

[14] R. Antia, S. S. Pilyugin, and R. Ahmed, Proc Natl Acad Sci U S A **95**, 14926 (1998).

[15] R. J. De Boer, D. Homann, and A. S. Perelson, J Immunol **171**, 3928 (2003).

[16] L. K. Selin et al., Immunity **11**, 733 (1999).

[17] L. K. Selin, K. Vergilis, R. M. Welsh, and S. R. Nahill, J Exp Med **183**, 2489 (1996).

[18] C. D. Surh and J. Sprent, Immunity **29**, 848 (2008).

[19] A. D. Judge, X. Zhang, H. Fujii, C. D. Surh, and J. Sprent, J Exp Med **196**, 935 (2002).

[20] N. Vrisekoop et al., Proc Natl Acad Sci U S A **105**, 6115 (2008).

[21] C. D. Surh and J. Sprent, Semin Immunol **17**, 183 (2005).

[22] C. Utzny and N. J. Burroughs, J Theor Biol **211**, 393 (2001).

[23] V. V. Ganusov and R. J. De Boer, Trends Immunol **28**, 514 (2007).

[24] S. P. Stromberg and J. Carlson, PLoS Comput Biol **2** (2006).

[25] E. Hammarlund et al., Nat Med **9**, 1131 (2003).

[26] L. Haynes, S. L. Swain, J. Cambier, and R. Fuldner, Mech. Ageing Dev. **126**, 822 (2005).

[27] R. A. Goldsby, T. J. Kindt, B. A. Osborne, and J. Kuby, *Immunology, Fifth Edition*, W. H. Freeman and Company, New York, 2003.

[28] A. S. Perelson and G. Weisbuch, Reviews of Modern Physics **69**, 1219 (1997), Copyright (C) 2008 The American Physical Society; Please report any problems to prola@aps.org.

[29] T. I. Workshop and A. S. Perelson, *Theoretical Immunology: The Proceedings of the Theoretical Immunology Workshop, Held June 1987, Santa Fe, New Mexico*, volume 2 of *Proceedings volume in the Santa Fe Institute studies in the sciences of complexity*, Addison-Wesley Pub. Co, Redwood City, Calif, 1987.

[30] T. I. Workshop and A. S. Perelson, *Theoretical Immunology: The Proceedings of the Theoretical Immunology Workshop, Held June 1987, Santa Fe, New Mexico*, volume 1 of *Proceedings volume in the Santa Fe Institute studies in the sciences of complexity*, Addison-Wesley Pub. Co, Redwood City, Calif, 1987.

[31] A. S. Perelson and G. F. Oster, Journal of theoretical biology **81**, 645 (1979), PMID: 94141.

[32] D. J. Smith, S. Forrest, R. R. Hightower, and A. S. Perelson, Journal of theoretical biology **189**, 141 (1997), PMID: 9405131.

[33] P. J. Linton and K. Dorshkind, Nat. Immunol **5**, 133 (2004).

[34] J. M. Carlson and J. Doyle, Phys. Rev. E **60**, 1412 (1999).

[35] J. M. Carlson and J. Doyle, Phys. Rev. Lett. **84**, 2529 (2000).

[36] J. Doyle and J. Carlson, Phys. Rev. Lett. **84**, 5656 (2000).

[37] J. Carlson and J. Doyle, Proc. Nat. Acad. Sci. **99**, 2538 (2002).

[38] M. Manning, J. M. Carlson, and J. Doyle, Phys. Rev. E **72**, 016108 (2005).

[39] M. A. Moritz, M. Morias, J. M. Carlson, and J. Doyle, Proc. Nat. Acad. Sci. **102**, 17912 (2005).

[40] M. D. Stubna and J. Fowler, Int. J. Bifurcation and Chaos **13**, 237 (2003).

[41] H. Geiger and G. V. Zant, Nat. Immunol **3**, 329 (2002).

[42] T. Zhou, J. M. Carlson, and J. Doyle, Proc. Nat. Acad. Sci **99**, 2049 (2002).

[43] T. Zhou, J. M. Carlson, and J. Doyle, J. Theor. Biol. **236**, 438 (2005).

[44] M. W. Deem and H. Y. Lee, Physical Review Letters **91**, 068101 (2003), Copyright (C) 2008 The American Physical Society; Please report any problems to prola@aps.org.

[45] S. F. de St. Groth and R. G. Webster, J. Exp. Med. **12**, 331 (1966).

[46] T. J. Kindt, B. A. Osborne, and R. A. Goldsby, *Kuby Immunology*, W. H. Freeman, 6 edition, 2006.

[47] A. G. Rolink, C. Schaniel, J. Andersson, and F. Melchers, Current Opinion in Immunology **13**, 202 (2001).

[48] G. Vieira and J. Chies, Medical Hypotheses **65**, 873 (2005).

[49] A. L. Rothman, The Journal of clinical investigation **113**, 946 (2004), PMID: 15057297.

[50] R. M. Welsh and R. S. Fujinami, Nature reviews. Microbiology **5**, 555 (2007), PMID: 17558423.

[51] A. B. SABIN, The American journal of tropical medicine and hygiene **1**, 30 (1952), PMID: 14903434.

[52] M. Alvarez et al., Am J Trop Med Hyg **75**, 1113 (2006).

[53] J. B. Beltman, A. F. M. Marée, J. N. Lynch, M. J. Miller, and R. J. de Boer, The Journal of experimental medicine **204**, 771 (2007), PMID: 17389236.

[54] C. Keşmir and R. J. D. Boer, Journal of immunology (Baltimore, Md. : 1950) **163**, 2463 (1999), PMID: 10452981.

[55] K. W. Wucherpfennig et al., Seminars in Immunology **19**, 216 (2007).

[56] M. B. Oldstone, *Molecular Mimicry: Infection Inducing Autoimmune Disease*, Springer, 1 edition, 2005.

[57] K. Naylor et al., J Immunol **174**, 7446 (2005).

[58] M. A. Nowak and R. May, *Virus dynamics: Mathematical principles of immunology and virology*, Oxford University Press, USA, 2001.

[59] L. W. Enquist, V. R. Racaniello, A. M. Skalka, and S. J. Flint, *Principles of Virology: Molecular Biology, Pathogenesis, and Control of Animal Viruses*, American Society Microbiology, 2 edition, 2000.

[60] World health organization fact sheet no. 117, 2009.

[61] S. Noisakran and G. C. Perng, Experimental Biology and Medicine (Maywood, N.J.) **233**, 401 (2008), PMID: 18367628.

[62] N. R. Klinman and J. L. Press, Transplantation reviews **24**, 41 (1975), PMID: 49962.

[63] A. R. Khaled and S. K. Durum, Nature reviews. Immunology **2**, 817 (2002), PMID: 12415306.

[64] J. Thakar, M. Pilione, G. Kirimanjeswara, E. T. Harvill, and R. Albert, PLoS computational biology **3**, e109 (2007), PMID: 17559300.